

## A late Permian palynological assemblage from the Spearfish Formation of South Dakota, United States: Implications for biostratigraphy, paleofloristics, and phytogeography

Carol L. Hotton <sup>a,\*</sup>, Antoine Bercovici <sup>b</sup>, Cindy V. Looy <sup>c</sup>, Ivo A.P. Duijnstee <sup>c</sup>, Dan S. Chaney <sup>a</sup>, Cortland F. Eble <sup>d</sup>, Isabel P. Montañez <sup>e</sup>, Sylvie Bourquin <sup>f</sup>, Blaine Cecil <sup>a<sup>1</sup></sup>, John Nelson <sup>g</sup>, Robert A. Gastaldo <sup>h</sup>, Johnathan Wingerath <sup>a</sup>, William A. DiMichele <sup>a</sup>

<sup>a</sup> Department of Paleobiology, National Museum of Natural History, Smithsonian Institution, Washington, DC 20560, United States

<sup>b</sup> Denver Museum of Nature & Science, 2001 Colorado Boulevard, Denver, CO 80205, USA

<sup>c</sup> Department of Integrative Biology, Museum of Paleontology, University of California-Berkeley, Valley Life Sciences Building #3140, Berkeley, California 94720, USA

<sup>d</sup> Kentucky Geological Survey, University of Kentucky, 247D Mining and Mineral Resources Bldg, Lexington, KY 40506, USA

<sup>e</sup> Department of Earth and Planetary Sciences, University of California, Davis, California 95616, USA

<sup>f</sup> Univ Rennes, CNRS, Géosciences Rennes - UMR 6118, F-35000 Rennes, France

<sup>g</sup> Illinois State Geological Survey, 615 E. Peabody Drive, Champaign, IL, 61820, USA

<sup>h</sup> Department of Geology, Colby College, Waterville, ME 04901, USA

### ARTICLE INFO

Editor: Howard Falcon-Lang

**Keywords:**

Spearfish Formation  
South Dakota  
Palynology  
Euramerica  
Lopingian  
Aridity  
Eolian dust

### ABSTRACT

We report here on a palynoflora from the Spearfish Formation of South Dakota that represents the first definite record of late Permian plant remains in the form of miospores from North America. The assemblage is dominated by taeniate pollen (*Lueckisporites virkkiae*, *Lunatisporites noviaulensis*, *Corisaccites alutus*, *Jugaspores spp.*) as well as simple saccate pollen taxa (*Klausipollenites schaubergeri*, *Falcisporites spp.*), but is highly depauperate in spores. The palynoflora was extracted from a mudstone associated with black fissile shales and carbonates about 30 m above the conformable contact with the underlying Minnekhata Limestone at Cascade Springs. Multiple lines of evidence from organic and carbonate petrology as well as acritarchs indicate that the depositional context was a brackish lagoon or inlet subject to high evaporation rates. Eolian dust, present in all studied units, combined with carbonate and organic petrography, indicates aridity through this interval. Through similarity and ordination analysis, we show that the Spearfish assemblage most closely resembles low paleolatitude palynofloras of late Permian (Lopingian) age in Europe and differs significantly from middle Permian palynofloras of the central United States. The palynoflora also differs from lower Triassic palynofloras, thereby establishing that the lower portion of the Spearfish Formation is late Permian. The similarity in composition of the Spearfish assemblage in the western United States to xeric European assemblages indicates that a near-uniform xerophytic flora dominated by voltzian conifers and peltasperms extended thousands of kilometers across low-latitude Pangaea in late Permian times.

### 1. Introduction

The Lopingian (late Permian) terrestrial world was a time of high provincialism, where strong temperature and precipitation gradients extended across the vast continent of Pangaea. Five distinct geographic phytoprovinces have been recognized, each characterized by a distinctive flora (Bernardi et al., 2017). The high northern latitude, cool temperate Angaran phytoprovince was dominated by cordaitalean seed

plants and pteridophytes, whereas the sub-Angaran contained a mixture of Angaran, Euramerican and Cathaysian elements (Meyen, 1982, 1987). The temperate southern hemisphere Gondwanan phytoprovince was dominated by glossopoterid seed plants, conifers and sphenophytes Archangelsky, 1990; Cuneo, 1996), and the island continent of Cathaysia was dominated by relict Pennsylvanian plants, as well as distinctive seed plants such as gigantopterids (Li and Yao, 1982; Wang, 1985; DiMichele et al., 2011). The broadly equatorial Euramerican

\* Corresponding author.

<sup>1</sup> deceased

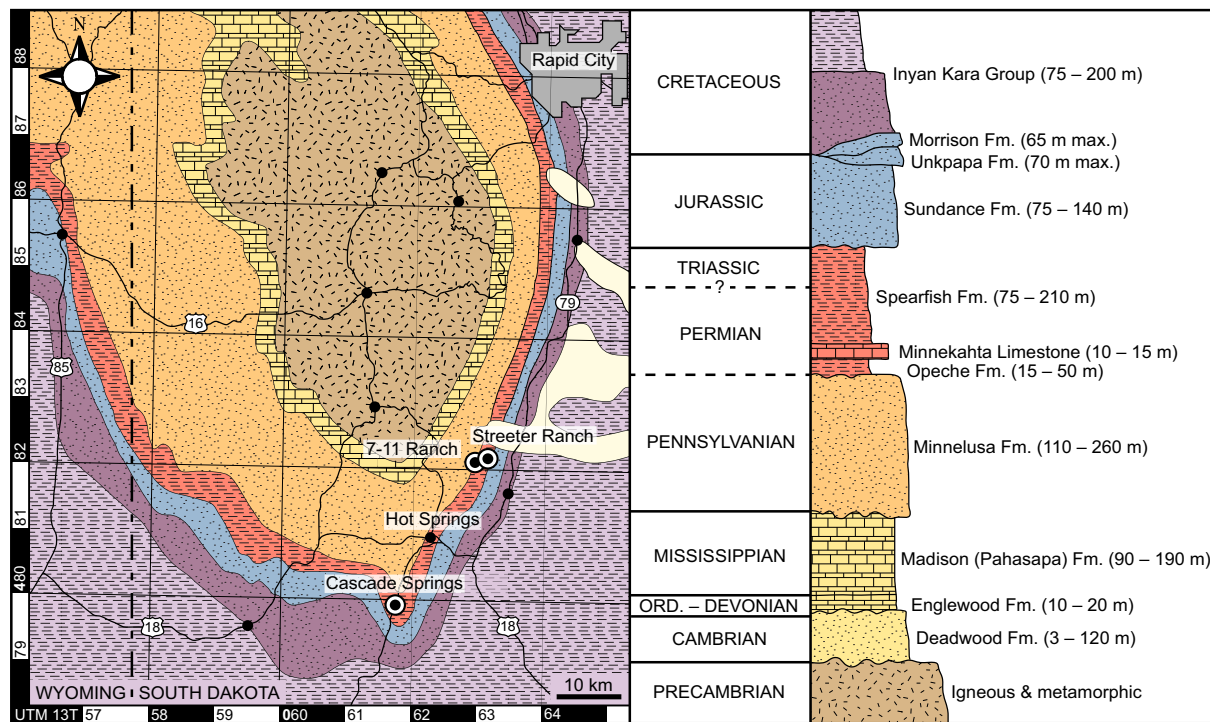


**Fig. 1.** Map of sampled Spearfish Formation localities in South Dakota, U.S.A. discussed in the context of the area's generalized geology and stratigraphy.

phytoprovince, extending across Europe and into the western Urals, was warm and dry, and was dominated by seed plants, including peltasperm and corytosperm seed ferns, ginkgophytes, voltzian conifers, putative cycadophytes, and subordinate spore-bearing sphenophytes (Schweitzer, 1986; Rees et al., 2002; DiMichele et al., 2008; Kustatscher et al., 2017; Uhl and Kerp, 2020). Our knowledge of floras of the Euramerican phytoprovince, although extensive, has been based solely on mega and microfossils from European and western Russian assemblages. Up to now, no plant remains in the form of either megafossils or palynomorphs have been definitely recorded from the late Permian of North America. The youngest megaflora known from North America, dominated by voltzian conifers, is probably early Roadian in age (DiMichele et al., 2004; Looy and Duijnstee, 2020).

In this report, we describe palynomorphs and their geological context from the Spearfish Formation of the Black Hills area of South Dakota. The samples were extracted from a distinctive laminated black shale/limestone unit in an otherwise monotonous sequence of red clastic rocks and gypsum beds. Our palynological data indicate that the gymnosperm-dominated floras of the Euramerican lowlands extended thousands of kilometers to the west in the late Permian. Endemism is surprisingly low in the Spearfish palynoflora, indicating that plant communities with a similar composition, undetected in the fossil record thus far, extended across a broad swath of mid-latitude North America. We explore the depositional environment of the black shale/limestone unit and its implications for interpretation of the depositional environment of the formation as a whole. Our data support the existence of a vast, relatively uniform terrestrial flora of relatively low diversity in the late Permian of Euramerica leading up to the end-Permian biotic crisis.

## 2. Geologic setting

The Black Hills are an outlier of the Rocky Mountains in the western Great Plains of South Dakota, U.S.A. Ovoid in outline, the hills have a core of Precambrian crystalline rocks surrounded by upturned sedimentary strata of Paleozoic and Mesozoic age. Like all the ranges of the Rocky Mountains, the Black Hills were uplifted during the last phase of the Laramide orogeny during Late Cretaceous and early Cenozoic times.

The outcrops where our collections were gathered are located south of the town of Hot Springs at the southern end of the Black Hills.

During the Permian, western South Dakota and most of Wyoming lay on a tectonically stable, passive continental margin bordered westward by a deep ocean basin in northern Utah and eastern Idaho. Within that basin, the peculiar phosphatic and cherty strata of the Phosphoria Formation accumulated. Eastward, the Phosphoria Formation grades to normal marine carbonate deposits of the Park City Formation, which in turn intertongues with redbeds and bedded gypsum of the Goose Egg (eastern Wyoming) and Spearfish (western South Dakota) formations. Reflecting stability of the cratonic platform, carbonate tongues of the Park City and Goose Egg formations have great lateral extent. Extending farthest east is the oldest limestone tongue, known as the Minnekahta Formation in the Black Hills, but recognized as the Minnekahta Limestone Member in Wyoming and correlative units to the west (Wardlaw and Collinson, 1986). The age of the Minnekahta Formation in South Dakota remains unconstrained (Stack and Gottfried, 2021); although correlative units to the west have been dated as late Kungurian (Behnken, 1975) or early Roadian (Wardlaw and Collinson, 1979), it is likely that the formation ranges into the early Wordian or even into the early Capitanian based on correlation with the Falcon Member in Colorado (Hagadorn et al., 2016). Although not formally established, it is likely that younger tongues of the Park City Formation transition eastward into gypsum beds of the Goose Egg and Spearfish formations (Boyd, 1993).

Darton first described the Spearfish Formation in the Black Hills region of South Dakota (Darton, 1899, 1901). It extends into Wyoming, Montana, Nebraska, and the subsurface of North Dakota. The formation rests conformably on the Minnekahta Formation, whereas its upper contact is defined by a major unconformity and is overlain by formations of Middle Jurassic age (Lindberg, 1988; Boyd, 1993; Johnson, 1993). The Spearfish Formation ranges in thickness from 136 to 250 m. In the southern Black Hills area it consists of four facies: 1) a lower red mudstone unit with thin gypsum lenses; 2) an evaporite facies of two to four beds of massive gypsum, up to 15 m thick, with lesser amounts of limestone, dolostone and red mudstone; 3) an upper mudstone facies; and 4) a cross-stratified sandstone-dominated facies at the top of the

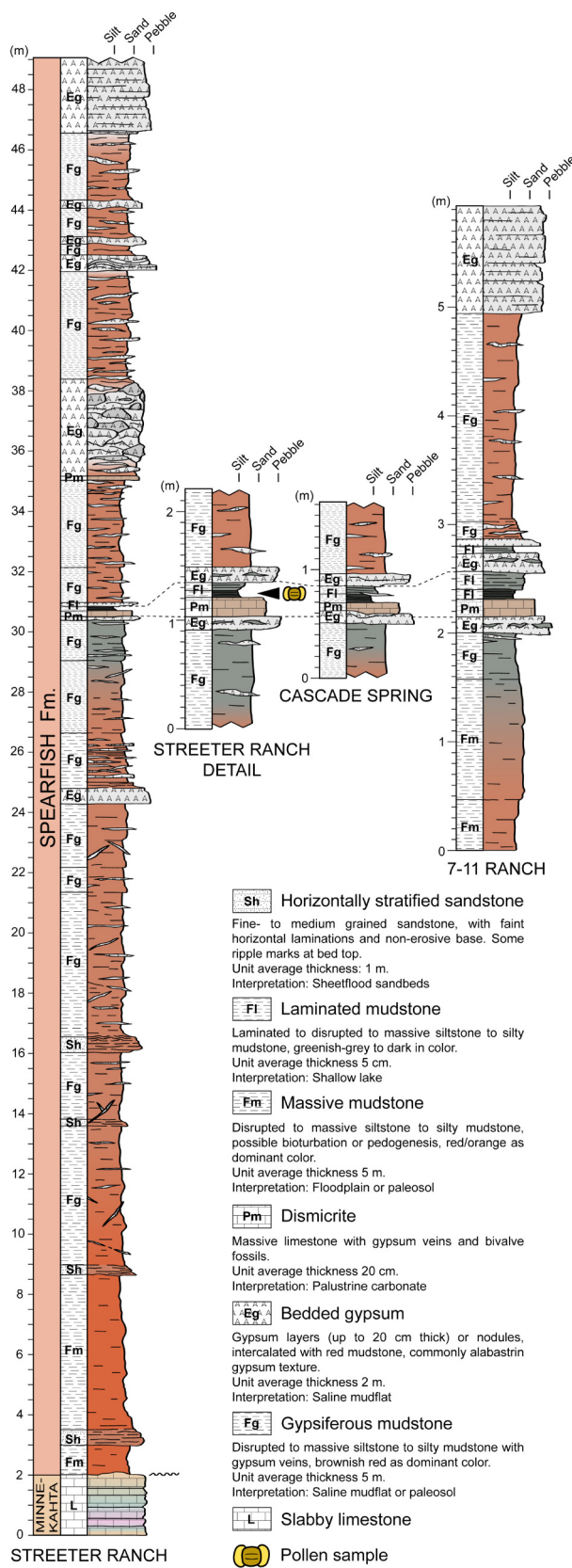


**Fig. 2.** Stratigraphic logs of sections discussed in text (Streeter Ranch: N43.52850°, W103.37729°; 7-11 Ranch: N43.52752°, W103.39320°; Cascade Springs: N43.3330°, W103.5492°). Pollen sample collected from laminated mudstone (arrow) at Cascade Springs. Vertical scale in meters.

formation (Johnson, 1993). The focus of our study is a lithologically distinctive bed near the base of the evaporite facies, comprising an indurated black, fissile shale and limestone bed (herein called the 'black shale bed'), described in more detail below.

The overall environmental setting of the Spearfish Formation has been interpreted as a low gradient marginal marine to supra-tidal sabkha, overlain by terrestrial deposits at its top. This interpretation is based on the presence of thick beds of massive to bedded gypsum, bedded dolostones and limestones, stromatolites and bivalve casts, desiccation cracks in mudstones, and flaser bedding (Sabel, 1984). Petrographic evidence of eolian dust in the 'black shale bed' and associated units, described below, support this interpretation.

The age of the Spearfish Formation is uncertain due to the absence of stratigraphically informative fossils: up to now only stromatolites and unidentifiable bivalve casts have been reported (Sabel, 1984). The evaporite facies of the Spearfish Formation has been informally correlated with upper marine carbonate tongues of the Goose Egg Formation in eastern Wyoming, the Park City Formation in western Wyoming, and the Phosphoria Formation and Park City Group of western Utah and eastern Nevada (Robinson et al., 1964; Behnken et al., 1986; Johnson, 1993; Wardlaw, 2015). Conodont faunas in these uppermost carbonate tongues suggest a latest Wordian age, based on the co-occurrence of *Merrillina divergens* and *Mesogondolella bitteri* (Wardlaw, 2015), although *M. bitteri* ranges up to the late Capitanian in west Texas (Henderson, 2018). The upper carbonate units of the Spearfish Formation have been correlated lithostratigraphically with the Dinwoody Formation of western Wyoming, which contains Early Triassic conodonts (Paull and Paull, 1983). Therefore, the Permian-Triassic boundary has been placed within the Spearfish Formation, although its precise position is uncertain. Johnson (1993) notes: "the Permian-Triassic contact probably lies somewhere in the upper part of the evaporite facies or in the lower part of the upper mudstone facies." However, until this report, no direct biostratigraphic or chronometric data have been available to support that inference.

### 3. Materials and methods

#### 3.1. Lithostratigraphic logs

The black shale bed is traceable for at least 20 km from a road cut on Highway 71 near Cascade Springs (N43.3330, W103.5492) to two outcrops to the north, 7-11 Ranch (N43.52752, W103.39320) and Streeter Ranch (N43.52850, W103.37729). Stratigraphic sections were measured at these three localities (Fig. 1). The Streeter Ranch section rests conformably on the underlying Minnekahta Formation and includes the lower two facies of the Spearfish Formation (Fig. 2). The other two measured sections focused on the black shale bed (Fig. 2) where, at Cascade Springs, it forms an undulating gray band above the red mudstone of facies 1 and above the lower bedded gypsum in facies 2 (Figs. 3A, B). Samples were collected from an underlying bed and sub-units composing the black shale bed. Further details are supplied in Section 4.1.

#### 3.2. Palynology

One productive pollen sample was collected at the Cascade Springs locality in 2011 from a dark gray mudstone immediately underlying the fissile black shale. An additional sample was collected from the same site in 2012. Both the gray mudstone and black fissile shale were macerated for pollen, but it proved very difficult to dissociate palynomorphs from amorphous organic debris in the latter without destroying the pollen; hence, only the clastic mudstone residue was counted for palynomorphs. Palynological samples were prepared by Global Geolab Ltd., Medicine Hat, Alberta, Canada using standard techniques (hydrofluoric and hydrochloric acid maceration, heavy liquid separation, sieving through a 10-µm mesh, and strew-mounting in Elvacite). Some residue also was

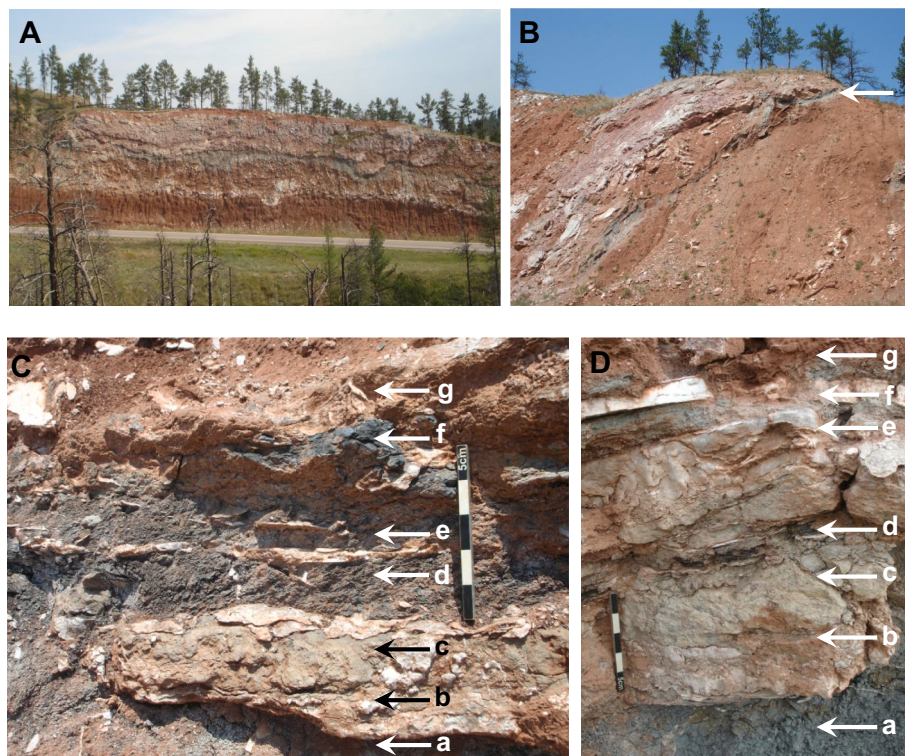


**Fig. 3.** Outcrop photographs. A. Exposure of Cascade Springs site showing, in ascending order, red mudstone facies, lower gypsum bed, and 'black shale bed' in middle of outcrop (prominent gray band). B. Exposure of Cascade Springs anticline (arrow indicates level from which pollen sample collected). C. 'Black shale bed' at Cascade Springs, showing in ascending order: gray blocky siltstone (a); a basal gypsum and carbonate bed (b); grading into a limestone (c); overlain by a gray mudstone (d); gypsum stringers (e); fissile black shale (f); and a capping red mudstone (g). Scale = 5 cm. D. 'Black shale bed' at 7-11 Ranch where arrows indicate, in ascending order: gray blocky siltstone (a); carbonate and gypsum bed (b); limestone (c); fissile black shale (d); upper carbonate unit (e); gypsiferous/Gy mudstone and thin 'alabaster' bedded gypsum (f); and red mudstone on top (g). Scale = 5 cm. (For interpretation of the references to colour in this figure legend, the reader is referred to the web version of this article.)

mounted in glycerin jelly. Specimens were observed with a Nikon Eclipse 80i compound microscope. Specimen locations were noted with an England Finder graticule. Recovery was relatively poor, and 13 slides were examined to achieve a count of 300 grains identifiable at least to genus. Palynomorph preservation varied from poor (badly corroded, fragmented and unidentifiable) to excellent (uncorroded, complete, identifiable to species). Palynomorphs were imaged with Differential Interference Contrast, a Plan Apo 63 $\times$  Oil objective, and a Nikon DXM1200F camera. Extended depth of field (EDF) images were generated using Adobe Photoshop CS 6 version 13.0. Microscope slides with illustrated specimens are stored in the U.S. National Museum of Natural History Paleobotanical Type and Illustrated Collections under catalog numbers USNM43663A – USNM43663M.

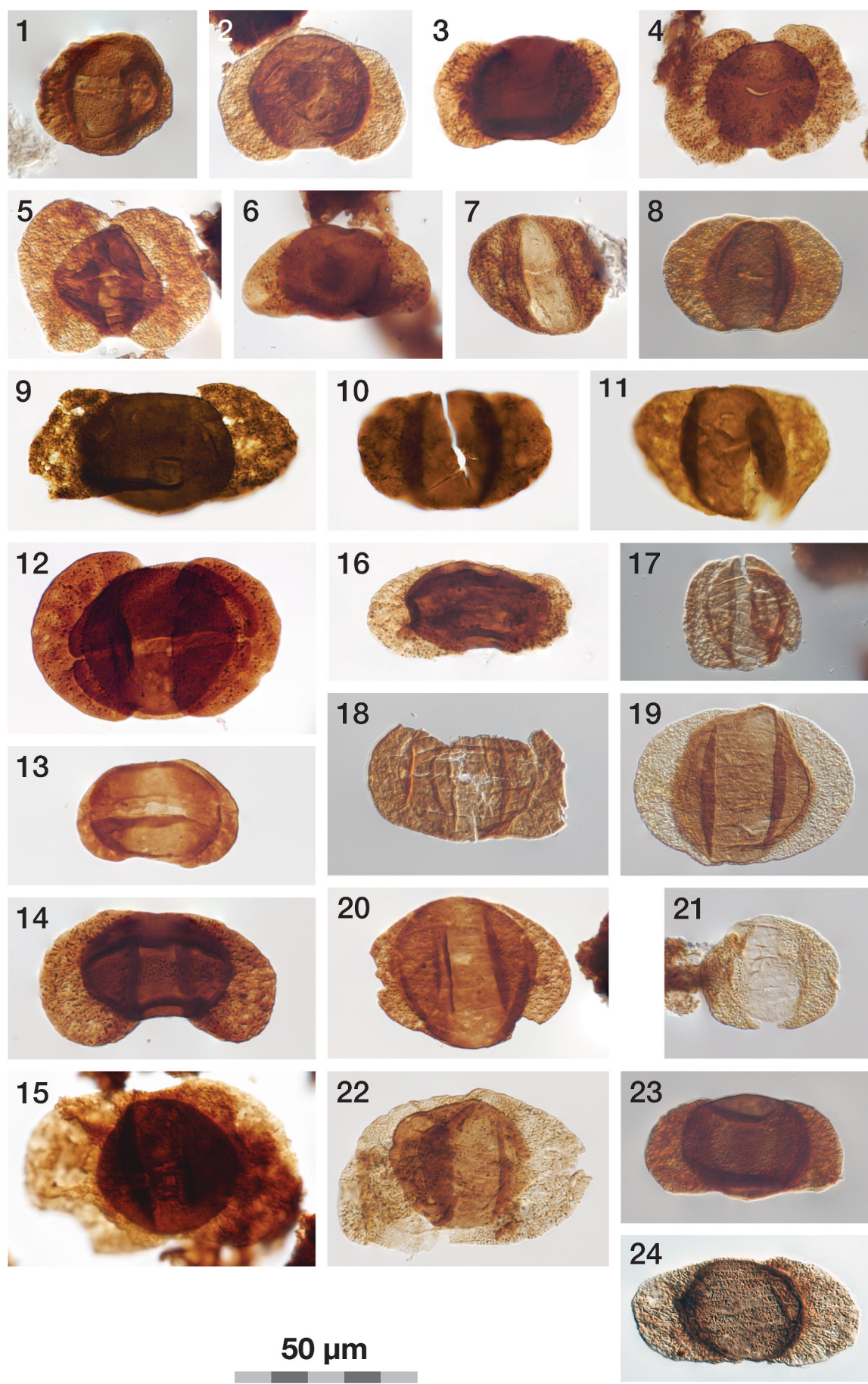
### 3.3. Ordination of palynological data

A database of 57 published European palynofloras and one North African palynoflora, all of Lopingian age, was compiled for comparison with the Spearfish palynoflora. For comparison, three middle Permian U.S. palynofloras were added to the database, as well as one U.S. and ten European palynofloras from the Triassic (Table S1). In compiling the data, homotypic synonyms were merged, but putative heterotypic synonyms were maintained as distinct. Together with the Spearfish assemblage, this resulted in a matrix of 458 palynomorph taxa by 73 palynofloras (including the Spearfish assemblage). To reconstruct approximate Lopingian paleogeographic positions of all the current palynological sample locations, we used GPlates Web Service (<http://gws.gplates.org>; see Müller et al., 2018). This provides reconstructed paleocoordinates estimates, based on the plate tectonic reconstruction model by Zahirovic et al. (2022).

Multivariate comparison between Spearfish and the other 72 palynofloras was approached in two different ways; both shown in the discussion section. The first comparative method considers the bilateral compositional similarity between the Spearfish assemblage and each of the other localities. From a wide range of available similarity/distance indices for binary data (see Choi et al., 2010, for an overview of 76 of those), Simpson similarity was selected because of its applicability for presence/absence data of potentially incomplete or undersampled assemblages. This similarity measure counts the number of matches between two assemblages and divides it by the number of taxa present in the smallest set (assuming that the smaller of the two assemblages poses the highest risk of being more incomplete). Thus, it treats two assemblages as being potentially identical if one is a subset of the other. The second approach compared the taxonomic composition of all samples simultaneously in a Detrended Correspondence Analysis (DCA). DCA is compatible with presence/absence data (Ter Braak, 1985), and aims to maximize the functional between-sample differences in the original data matrix along just a few dimensions, while allowing for a unimodal response of taxon presence along very long environmental gradients or very long temporal records. The initial CA ordination that forms the basis of the DCA was detrended using 26 segments. All analyses were performed using the paleontological statistical software package Past 4 (Hammer and Harper, 2001).

### 3.4. Black shale geochemistry

A shale split was reduced in size to  $-60$  mesh (upper size limit, 250  $\mu\text{m}$ ) and total carbon and sulfur were determined using a Leco SC-432 carbon/sulfur analyzer. Inorganic carbon was determined using a UIC CM 5014 coulometer. The total organic carbon (TOC) content was



(caption on next page)

**Fig. 4.** Spearfish assemblage: taeniate pollen, in alphabetical order. USNM accession number (slide #): EF = England Finder Coordinate. 1. *Corisaccites alutus* Venkatachala & Kar 1966: accession USNM 43663D (slide # SD2012-02-22): EF R38. 2. *Jugasporites delasaucei* (Potonié & Klaus) Leschik 1956: accession USNM 43663 M (slide # SD06112011.3-20): EF O31. 3. *Jugasporites latus* (Leschik) Foster 1983: accession USNM 43663G (slide # SD06112011.3-2.5): EF Q38/1. 4. *Jugasporites nubilus* Leschik 1956: accession USNM 43663E (slide # SD2012-02-3b-1): EF J46/3. 5. *Jugasporites* sp. cf. *J. nubilus*: accession USNM 43663 M (slide # SD06112011.3-20): EF S45. 6. *Jugasporites paradelasaucei* Klaus, 1963: accession USNM 43663 M (slide # SD06112011.3-20): EF J31/3. 7. *Labiisporites granulatus* Leschik 1956: accession USNM 43663C (slide # SD2012-02-3b-21): EF F27. 8. *Limitisporites rectus* Leschik 1956: accession USNM 43663 L (slide # SD06112011.3-19): EF L22/3. 9. *Limitisporites lepidus* (Luber & Valts) Hart 1965: accession USNM 43663C (slide # SD-2012-02-3b-21): EF D39. 10. *Limitisporites moersensis* (Grebe) Klaus, 1963: accession USNM 43663 L (slide # SD06112011.3-19): EF L34/3. 11. *Limitisporites parvus* Klaus, 1963: accession USNM 43663 K (slide # SD06112011.3-6): EF X37. 12. *Lueckisporites virkkiae* Potonié & Klaus 1954: accession USNM 43663G (slide # SD06112011.3-6): EF J41/1. 14. *Lunatisporites noviaulensis* (Leschik) Foster 1979: accession USNM 43663G (slide # SD06112011.3-2.5): EF H29. 15. *Lunatisporites pantii* (Jansonius) Orlowska-Zwolińska 1984: accession USNM 43663 L (slide # SD06112011.3-19): EF O38/3. 16. *Protohaploxylinus haigii* Foster 1979: accession USNM 43663B (slide # SD2012-02-3b-20): EF Q38/4. 17. *Protohaploxylinus hartii* Foster 1979: accession USNM 43663 L (slide # SD06112011.3-19): EF H48/2. 18. *Protohaploxylinus limpidus* (Balme & Henneley) Balme & Playford 1967: accession USNM 43663 L (slide # SD06112011.3-19): EF S25/1. 19. *Protohaploxylinus microcorpus* (Schaarschmidt) Clarke 1965: accession USNM 43663D (slide # SD2012-02-22): EF X30/3. 20. *Protohaploxylinus* sp. cf. *P. suchonensis* (Schaarschmidt) Clarke 1965: accession USNM 43663G (slide # SD06112011.3-2.5): EF Q36/2. 21. *Protohaploxylinus* sp. 1b: accession USNM 43663C (slide # SD2012-02-3b-21): EF U46/2. 22. *Protohaploxylinus* sp. 3: accession USNM 43663B (slide # SD2012-02-3b-20): EF T38. 23. *Scutasperites unicus* Klaus, 1963: accession USNM 43663E (slide # SD06112011.3-1): EF V45. 24. *Striatobiteites richteri* (Klaus) Hart 1964: accession USNM 43663 A (slide # SD2012-02-3b-1): EF D32/2.

determined by difference where:

$$\text{Total Organic Carbon (TOC)} = \text{Total Carbon (TC)} - \text{Total Inorganic Carbon (TIC)}$$

### 3.5. Black shale petrography

Black shale samples from the Streeter Ranch locality were placed in 7.6 cm diameter phenolic ring forms, and covered with epoxy resin. Once cured, the samples were ground and polished using 320, 400, and 600 grit papers, 1.0, 0.3, and 0.05  $\mu\text{m}$  alumina suspensions, and colloidal silica as a final polishing compound. Polished mounts were examined in white and UV fluorescent reflected light on a Zeiss UEM microscope, using a 40 $\times$  epiplan oil immersion objective. Fluorescent light analysis was achieved using a mercury arc light source in conjunction with Zeiss CZ709 FITC filter set (450–490 nm emission filter, 510 nm beam-splitter, 515 nm emission filter).

### 3.6. Carbonate petrography and stable isotope analysis

Nine representative samples of the limestone from the 7–11 Ranch locality were analyzed petrographically by transmitted light. Three samples were microsampled using a Merchantek computer-driven drill with a 50  $\mu\text{m}$  diamond-tip drill bit, and analyzed for their carbon-and-oxygen isotope compositions: a carbonate micrite (S1A1), and microbial micropeloidal clasts from S1A2 and S1B2. Microdrilled samples (60 to 100  $\mu\text{g}$ ) were heated at 375° F in vacuo to remove organic volatiles.  $\delta^{18}\text{O}$  and  $\delta^{13}\text{C}$  values were determined using a Fisons Optima IRMS with a 90 °C Isocarb common acid-bath autocarbonate system in the Stan Margolis Stable Isotope Lab, UC Davis. Analytical precision for both  $\delta^{18}\text{O}$  and  $\delta^{13}\text{C}$  is  $<\pm 0.1\text{ ‰}$  ( $1\sigma$ ). All stable isotope values are reported relative to Pee Dee Belemnite (PDB) using standard delta notation.

### 3.7. Thin sections of rock units

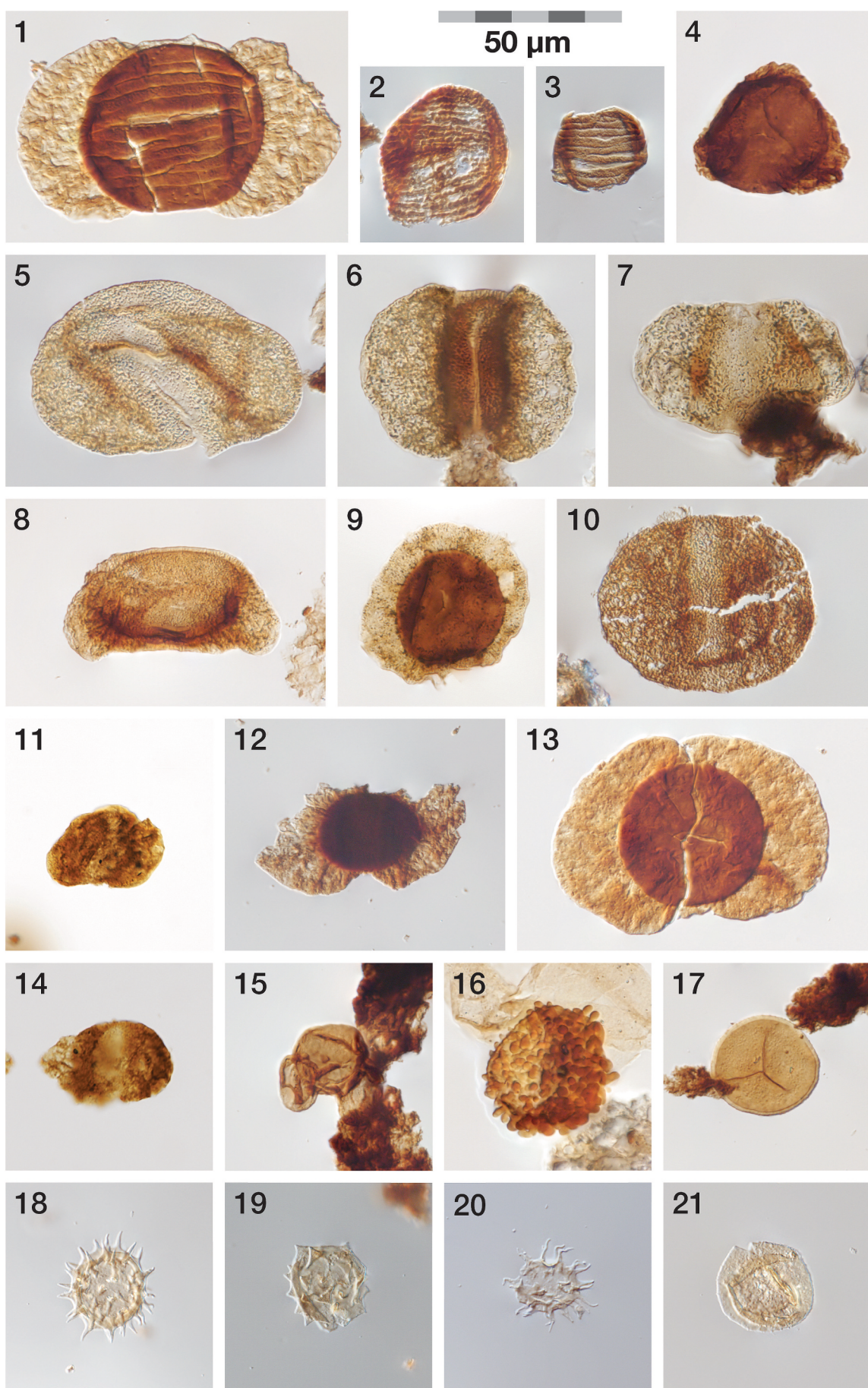
Thin sections were made of each unit comprising the black shale bed as well as the underlying gray siltstone. As needed, the samples were trimmed to fit a cross section of each on a standard 1" x 2" petrographic slide. The samples were placed in latex molds that were filled with epoxy. Embedment of the samples was enhanced by placing the samples in the molds in a vacuum chamber, which was maintained at ~38 Torr for 5 min. After the epoxy blocks containing the samples had cured overnight, they were removed from the latex molds. Each was ground on wet 320 grit silicon carbide paper until a good cross section was

exposed. Due to low porosity, the epoxy did not completely penetrate the samples. The freshly exposed shale surfaces of the blocks were generously coated with epoxy and placed in the vacuum chamber again. Upon removal from the vacuum chamber, the blocks were placed with the fresh epoxy side down onto a sheet of mylar and allowed to cure overnight. The mylar was removed from the blocks, and the working faces ground with 320, 600, and 1200 grit sandpaper. The working faces of the blocks were coated again with epoxy, placed in the vacuum chamber for 5 min at ~40 Torr, removed and adhered to glass slides. Once the epoxy had cured, excess epoxy was trimmed from the edges of the slides. Sections were cut from the blocks and initial grinding accomplished using a Hillquist thin-sectioning machine. Final grinding of the thin-sections was accomplished by hand using wet 320, 600, and 1200 grit sandpaper on plate glass. The thin sections were polished using a Leco SS-1000 Spectrum System Grinder Polisher equipped with an 8 in., Buehler Microcloth Polishing Cloth catalog No. 40-7218 from Buehler, Lake Bluff Illinois, and 03  $\mu\text{m}$  Alpha Alumina polishing compound also from Leco Corporation, St. Joseph Michigan. The thin sections were examined using a Nikon Optiphot2-POL petrographic microscope and imaged with a Nikon DS-Fi3 colour camera under crossed Nicols and captured with NIS Elements-D software.

## 4. Results

### 4.1. Description of black shale bed

The following description is based on observations from the three measured sections, which vary only in minor detail. The black shale bed interval is underlain by a basal red mudstone grading into a medium gray, blocky siltstone ranging from 250 to 750 cm in thickness (Figs. 3C(a), 3D(a)). This gray siltstone grades vertically into a bed of thin gypsum and limestone, expressed as lenses, about 10 cm thick with an erosive upper contact (Figs. 3C(b), 3D(b)). The overlying unit is an indurated, highly contorted limestone, ranging from 12 to 15 cm thick, with gypsum lenses near the top (Figs. 3C(c), 3D(c)). These grade vertically into a black, indurated, highly carbonaceous, fissile shale 5–7 cm thick (Figs. 3C(d), Figs. 3D(d)). Separating the limestone and the black shale is a very thin, laminated, dark gray mudstone less than 1 cm thick, the source of the palynomorphs (not visible in photographs). A second layer of highly contorted limestone is locally present above the fissile black shale (Figs. 3C(e), 3D(e)); it grades up section into gray laminated siltstone and bedded gypsum (Figs. 3C(f), 3D(f)) overlain by red mudstone (Figs. 3C(g), 3D(g)).



(caption on next page)

**Fig. 5.** Spearfish Palynoflora: Taeniate and non-taeniate pollen, spores, acritarchs, in alphabetical order. USNM accession number (slide #): EF = England Finder Coordinate. 1. *Stroterporites jansoni*<sup>ii</sup><sup>Klaus, 1963</sup>: accession USNM 43663H (slide # SD06112011.3–3): EF U44. 2. *Vittatina costabilis*<sup>ii</sup><sup>Wilson, 1962</sup>: accession USNM 43663 L (slide # SD06112011.3–19): EF T23. 3. *Vittatina* sp. cf. *V. heclae*<sup>Uutting, 1994</sup>: accession USNM 43663 M (slide # SD2012–02–3b–22): EF T36. 4. *Fuldaesporites* sp.: accession USNM 43663B (slide # SD2012–02–3b–20): EF D30. 5. *Falcisporites rughallensis* (Clarke) Balme 1970: accession USNM 43663 M (slide # SD2012–02–3b–22): EF W29. 6. *Falcisporites stabilis* Balme 1970: accession USNM 43663D (slide # SD2012–02–3b–22): EF Q46/3. 7. *Falcisporites zapfei* (Potonié & Klaus) Leschik 1956: accession USNM 43663B (slide # SD2012–02–3b–20): EF X16/1. 8. *Klausipollenites schaubergeri* (Potonié & Klaus) *Jansonius, 1962*: accession USNM 43663G (slide # SD06112011.3–2.5): EF Q37/4. 9. *Nuskisporites* sp.: accession USNM 43663 A (slide # SD2012–02–3b–1): EF Q40/1/3. 10. *Paravescaspora splendens* (Leschik) *Klaus, 1963*: accession USNM 43663C (slide # SD2012–02–3b–21): EF U28. 11. *Pityosporites devolvens* Leschik 1955: accession USNM 43663 L (slide # SD06112011.3–19): EF E22/4. 12. *Platysaccus papilionis* Potonié & Klaus 1959: accession USNM 43663E (slide # SD06112011.3–1): EF F28/3. 13. *Rhizomaspora radiata*<sup>ii</sup><sup>Wilson, 1962</sup>: accession USNM 43663 K (slide # SD06112011.3–6): EF E38. 14. *Vesicaspora* sp. cf. *V. schemelli*<sup>ii</sup><sup>Klaus, 1963</sup>: accession USNM 43663 L (slide # SD06112011.3–19): EF O31/2.15. Bisaccate genus A: accession USNM 43663G (slide # SD06112011.3–2.5): EF S44/3. 16. *Clavatasporites irregularis*<sup>ii</sup><sup>Wilson, 1962</sup>: accession USNM 43663D (slide # SD2012–02–3b–22): EF W20/1. 17. *Cyclogranisporites* sp.: accession USNM 43663G (slide # SD06112011.3–2.5): EF Q27/3. 18. *Micrhystridium breve*<sup>ii</sup><sup>Jansonius, 1962</sup>: accession USNM 43663E (slide # SD06112011.3–1): EF K20/1. 19. *Micrhystridium* sp. 2: accession USNM 43663E (slide # SD06112011.3–1): EF H45/4. 20. *Multiplicisphaeridium* sp.: accession USNM 43663G (slide # SD06112011.3–2.5): EF J19/4. 21. *Leiosphaeridia* sp.: accession USNM 43663E (slide # SD06112011.3–1): EF T12/U12.

## 4.2. Palynology

Identification to species level was challenging due to variable preservation, but a sufficient subset of well-preserved grains allowed characterization of the Spearfish assemblage. It is dominated by taeniate bisaccates, comprising about 73 % out of the total of a 300-grain count. Non-taeniate bisaccates comprise about 25 % of the total. Other pollen species (taeniate non-saccates, monosaccates and trisaccates) make up less than 2 % of the total, and spores comprise less than 1 % of the total. The single most common species is the taeniate bisaccate *Lueckisporites virkkiae* (Fig. 4.12), consisting of 20 % of the total, followed by *Klausipollenites schaubergeri* (Fig. 5.8), and *Lunatisporites noviaulensis* (Fig. 4.14), each comprising 10 % of the total. Other important taxa include *Falcisporites* spp. (Figs. 5.4–5.6), *Jugasporites* spp. (Figs. 4.2–4.6), especially *Jugasporites delasaucei* (Fig. 4.6), *Limitisporites* spp. (Figs. 4.8–4.11), and *Corisaccites alatus* (Fig. 4.1). Less common components include several species of *Protohaploxylinus* (Figs. 4.16–4.22) *Vittatina costabilis* (Fig. 5.2), *Scutasperites uniculus* (Fig. 4.23), *Stroterporites jansoni* (Fig. 5.1), and *Vesicaspora* sp. (Fig. 5.14). Approximately 36 distinct morphotaxa are recognized. Notably, only two spore taxa, *Clavatasporites irregularis* (Fig. 5.16) and *Cyclogranisporites* sp. (Fig. 5.17), consisting of one specimen each were encountered in a 300-grain count. (See Table 1 for a complete list of taxa).

In addition to terrestrial palynomorphs, a very low diversity acritarch assemblage is present. These are represented by at least two morphospecies of *Micrhystridium* (Figs. 5.18–5.19), *Multiplicisphaeridium* sp. (Fig. 5.20), and *Leiosphaeridia* (Fig. 5.21). *Micrhystridium* species outnumbered pollen and spores by approximately 3:1, and *Leiosphaeridia* outnumbered pollen and spores by about 7:1. All species encountered at least once in the assemblage (excepting most in open taxonomy) may be found in Fig. 4 and Fig. 5.

## 4.3. Black shale petrology and geochemistry

Three polished blocks were examined petrographically. All were strongly dominated by lamalginite (the maceral term for thin, laminar algal material), comprising ≥95 % compared to other types of maceral. In some instances, lamalginite was found to grade into fluorescing bituminite (Fig. 6A), with bituminite representing mainly degraded algal material (Teichmüller, 1974). In reflected white light, lamalginite appears as an indistinct brown-black groundmass. However, in UV light, it exhibits a moderate-yellow fluorescence with distinctive banding (Figs. 6A,B). Other rarely observed liptinite macerals include resinite (Fig. 6C) and telalginite (Fig. 6D). Land-plant spores are present, but rare (for example, Fig. 6E). Inertodetrinitite (Fig. 6A) and vitrodetrinitite (Fig. 6B) occur only as very small (usually <10 µm), highly dispersed fragments. Inorganic matter is dominated by clay minerals, with quartz

grains of silt size dispersed throughout the matrix (Fig. 6F). Most of the clay matrix is coated with lamalginite. Thin, lighter-colored bands contain a higher proportion of quartz. Pyrite is present mainly as small euhedral crystals, with some frambooids (Fig. 6F). Small calcite (dolomite?) crystals also are also present in minor amounts.

Vitrinite reflectance values for two black shale samples are 0.36 and 0.38, respectively, placing them at, or very close to, the lignite/subbituminous C coal-rank boundary (Table 2A). The vitrinite particles are very small (< 20 µm), and comprise only a small fraction of the organic material. The dominant organic material is largely lamalginite. With a mineral matter content of 55.6 %, the black laminated shale is close to coal, a lithology that contains <50 % inorganic material by weight (Table 2B). The high volatile matter content (43.5 %) reflects the fact that the organic matter is almost entirely of algal origin (Table 2B).

## 4.4. Carbonate petrology

Samples examined range from bioturbated mudstone (SD3B) to phylloid algal packstone intercalated with carbonate micritic lamina (S1A1, S1B1), to micropeloidal mudstone exhibiting clotted micritic textures and intercalated with peloidal and skeletal wackestone (S1B2). *Archeolithophyllum* is observed in the micropeloidal mudstone, but replacement by anhydrite renders positive identification difficult. Skeletal components include ostracods, molds (steinkerns) of small planispiral gastropods and other molluscs ranging up to 2 cm in size.

Some samples are highly brecciated with clasts consisting predominantly of micropeloidal mudstone/wackestone (SB1; SD3A and SD3B). Primary (pores and skeletal steinkerns) and secondary porosity created by brecciation is occluded by gypsum cement and secondarily calcite spar (S1A2; S1BTop). The presence of relict anhydrite crystals in the gypsum cement indicates that the gypsum is a replacement of anhydrite. Sample SD313 shows signs of mild pedogenesis.

## 4.5. Carbonate stable isotope compositions

All microsampled carbonate components exhibit a narrow range of  $\delta^{18}\text{O}$  values (+2.8 to +4.7 ‰) that are substantially more  $\delta^{18}\text{O}$ -enriched than Phanerozoic marine carbonates that formed in normal salinity (3.5 ‰) seawater (Table 3). Conversely, the  $\delta^{13}\text{C}$  values show a larger range (−5.7 to 1.12 ‰) with phylloid algal packstone having significantly more  $\delta^{13}\text{C}$ -depleted values (−5.7 ‰ ± 0.3 ‰) than the micropeloidal mudstone/wackestone (−1.7 to −1.2 ‰) (Table 3).

## 4.6. Description of thin sections

In thin section, all of the units in the black shale bed contain silt-sized quartz grains interpreted as eolian dust. Virtually all quartz grains

**Table 1**  
Pollen Count by Taxon ( $N = 300$ ).

Taxon	Number	Percentage
<i>Clavatasporites irregularis</i> Wilson, 1962	1	0.33
<i>Corisaccites altutus</i> Venkatachala & Kar 1966	9	3.00
<i>Cyclogranisporites</i> sp.	1	0.33
<i>Falcisporites nuthallensis</i> (Clarke) Balme 1970	4	1.33
<i>Falcisporites stabilis</i> Balme 1970	6	2.00
<i>Falcisporites</i> sp. cf. <i>F. stabilis</i> Balme 1970	3	1.00
<i>Falcisporites zapfei</i> (Potonié & Klaus) Leschik 1956	3	1.00
<i>Falcisporites</i> sp. cf. <i>F. zapfei</i> (Potonié & Klaus) Leschik 1956	3	1.00
<i>Fuldaesporites</i> sp.	1	0.33
<i>Jugasporites delasaucei</i> (Potonié & Klaus) Leschik 1956	8	2.67
<i>Jugasporites latus</i> (Leschik) Foster 1983	15	5.00
<i>Jugasporites nubilus</i> Leschik 1956	4	1.33
<i>Jugasporites</i> sp. cf. <i>J. nubilus</i> Leschik 1956	11	3.67
<i>Jugasporites paradelasaucei</i> Klaus, 1963	1	0.33
<i>Jugasporites</i> spp. indeterminate	3	1.00
<i>Klausipollenites schaubergeri</i> (Potonié & Klaus) Jansonius, 1962	33	11.00
<i>Labiisporites granulatus</i> Leschik 1956	4	1.33
<i>Limitisporites lepidus</i> (Luber & Vals) Hart 1965	9	3.0
<i>Limitisporites parvus</i> Klaus, 1963	1	0.33
<i>Limitisporites rectus</i> Leschik 1956	2	0.67
<i>Limitisporites moersensis</i> (Grebe) Klaus, 1963	2	0.67
<i>Limitisporites</i> spp. indeterminate	7	2.33
<i>Lueckisporites parvus</i> Klaus, 1963	2	0.67
<i>Lueckisporites virkkiae</i> Potonié & Klaus 1954	64	21.33
<i>Lueckisporites</i> sp. cf. <i>L. virkkiae</i> Potonié & Klaus 1954	3	1.00
<i>Lueckisporites</i> spp. indeterminate	8	2.67
<i>Lunatisporites noviaulensis</i> (Leschik) Foster 1979	35	11.67
<i>Lunatisporites partii</i> (Jansonius) Orlowska-Zwolińska 1984	1	0.33
<i>Lunatisporites</i> spp. indeterminate	7	2.33
<i>Nuskisporites</i> sp.	1	0.33
<i>Paravesicaspora splendens</i> (Leschik) Klaus, 1963	2	0.67
<i>Pityosporites devolvens</i> Leschik 1955	1	0.33
<i>Platysaccus papillionis</i> Potonié & Klaus 1959	1	0.33
<i>Platysaccus</i> spp. indeterminate	6	2.00
<i>Protohaploxylinus haigii</i> Foster 1979	2	0.67
<i>Protohaploxylinus hartii</i> Foster 1979	1	0.33
<i>Protohaploxylinus limpidus</i> (Balme & Henneley) Balme & Playford 1967	2	0.67
<i>Protohaploxylinus microcorpus</i> (Schaarschmidt) Clarke 1965	1	0.33
<i>Protohaploxylinus</i> sp. cf. <i>P. suchonensis</i> (Schaarschmidt) Clarke 1965	1	0.33
<i>Protohaploxylinus</i> spp. indeterminate	4	1.33
<i>Rhizomaspis radiata</i> Wilson, 1962	1	0.33
<i>Scutasperites uniculus</i> Klaus, 1963	8	2.67
<i>Scutasperites</i> sp. cf. <i>S. uniculus</i> Klaus, 1963	2	0.67
<i>Striatobabites richteri</i> (Klaus) Hart 1964	1	0.33
<i>Striatobabites</i> sp. cf. <i>S. richteri</i> (Klaus) Hart 1964	2	0.67
<i>Strotersporites jansonii</i> Klaus, 1963	2	0.67
<i>Vesicaspora</i> sp. cf. <i>V. schemelii</i> Klaus, 1963	3	1.0
cf. <i>Vesicaspora</i> sp.	4	1.33
<i>Vittatina costabilis</i> Wilson, 1962	1	0.33
<i>Vittatina</i> sp. cf. <i>V. heclae</i> Utting, 1994	1	0.33
<i>Vittatina</i> sp. indeterminate	1	0.33
Bisaccate genus A	1	0.33
TOTAL	300	100.00

exhibit some degree of surface corrosion and/or chert overgrowth. Etched quartz grains are especially evident in the underlying gray siltstone (Fig. 7A) and in the pollen-producing mudstone (Fig. 7B).

## 5. Discussion

### 5.1. Palynostratigraphic evidence for the age of the Spearfish Formation

In order to establish the age of the Spearfish assemblage, we compared its composition to 67 palynofloras from Europe (57 from the Lopingian plus 10 from the Early Triassic), one north African assemblage (Lopingian), and four representing central U.S. localities, three of early middle Permian age (Guadalupian) and one from the Early Triassic. Details of these palynological assemblages are found in Table S1. When

the similarities of all palynofloras with the Spearfish assemblage are viewed in their paleogeographic context (Fig. 8A), what stands out is the affinity of the Spearfish palynoflora with central, western and southwestern European assemblages from the Lopingian, as opposed to the geographically proximate older and younger palynofloras. Of course, around the end of the Paleozoic, the Spearfish locality and Europe were on the same central Pangaea land mass and apart by only half their current distance, but they were nonetheless separated by 55° of equatorial longitude. Both paleogeographical distance to the spearfish locality and paleolatitude turn out to be poor predictors of palynofloral similarity to the Spearfish assemblage (Fig. 8B, C), in sharp contrast to the age of the palynofloras: higher Simpson similarities (i.e., well above 0.3) are exclusively found in comparisons with the Lopingian palynofloras (Fig. 8D). Seventy-four percent (74 %) of these Lopingian assemblages had higher similarities with Spearfish than any of the 14 younger or older palynofloras, strongly supporting a Lopingian age for the Spearfish assemblage.

Results of our ordination confirm this interpretation, placing the Spearfish assemblage firmly within a cluster of Lopingian assemblages of the Euramerican phytoprovince (Fig. 8E, F). The most prominent type of assemblage variation in the data set, captured by the first DCA axis, almost perfectly separates the Triassic assemblages from their Permian counterparts, while the second largest source of variance (DCA axis 2) largely concerns the type of variation found between assemblages from the Guadalupian and the younger assemblages. On DCA axis 3, the Early Triassic and Guadalupian assemblages (which formed the outliers on the first axis) line up because they do not share the type of variation that is recorded on this axis (i.e., mostly representing a type of Lopingian intra-European floral variability). Because the explanatory power of subsequent DCA axes decreases, the type of compositional similarities among Guadalupian and Early Triassic assemblages captured by third axis can be considered subordinate to the differences highlighted by the first axis.

There is considerable scatter in the DCA of the Lopingian European samples, but within that cluster, the Spearfish assemblage appears closest to those described from areas in Central and Western Europe—just as suggested by the similarity analysis (Fig. 8A). Linking these floras are some less common taxa, including *Jugasporites latus*, *Limitisporites moersensis*, *Lueckisporites parvus*, *Scutasperites uniculus*, *Strotersporites jansonii*, and *Vittatina costabilis*. Other similar assemblages include those from Italy, Germany, Spain, France, Poland, the Netherlands and Algeria, linked with the Spearfish by the presence of *Falcisporites zapfei*, *Jugasporites delasaucei*, *Klausipollenites schaubergeri*, *Lueckisporites virkkiae*, and *Paravesicaspora splendens*; and to a lesser extent *Limitisporites* sp., *Nuskisporites* sp., *Protohaploxylinus* spp., and specifically *Protohaploxylinus microcorpus*. Indeed, most of the European assemblages cluster together to some degree. Species of *Gardenasperites*, *Gigantosporites*, *Ephedripites* and *Striatopodocarpidites*, which are relatively common in Lopingian European palynofloras, are notably absent from the Spearfish assemblage. If these latter taxa are present in the South Dakota, they occur below the level detectable in our count. The Spearfish assemblage is also notable in the rare occurrence of Gondwanan and sub-Angaran elements; these include *Protohaploxylinus haigii*, *P. hartii*, *Limitisporites lepidus*, and *Vittatina heclae*, which are absent from European assemblages.

As noted, the Spearfish assemblage is quite distinct from early Triassic palynofloras. Moreover, characteristic Early Triassic lycopid spore taxa, such as *Densisporites*, *Endosporites*, *Lundbladispora*, and *Krauselisporites* (Kürschner and Herngreen, 2010; Nowak et al., 2018), were not observed in the Spearfish assemblage. Although some late Permian taxa, such as species of *Lunatisporites*, *Strotersporites*, and *Protohaploxylinus*, do range into the Early Triassic in low numbers, their abundance in the Spearfish assemblage, as well as the absence of characteristic Early Triassic spore taxa, further strongly supports a late Permian age assignment.

Three Permian assemblages from the El Reno Group in Oklahoma, U.S.A., were included in the comparative analyses because their

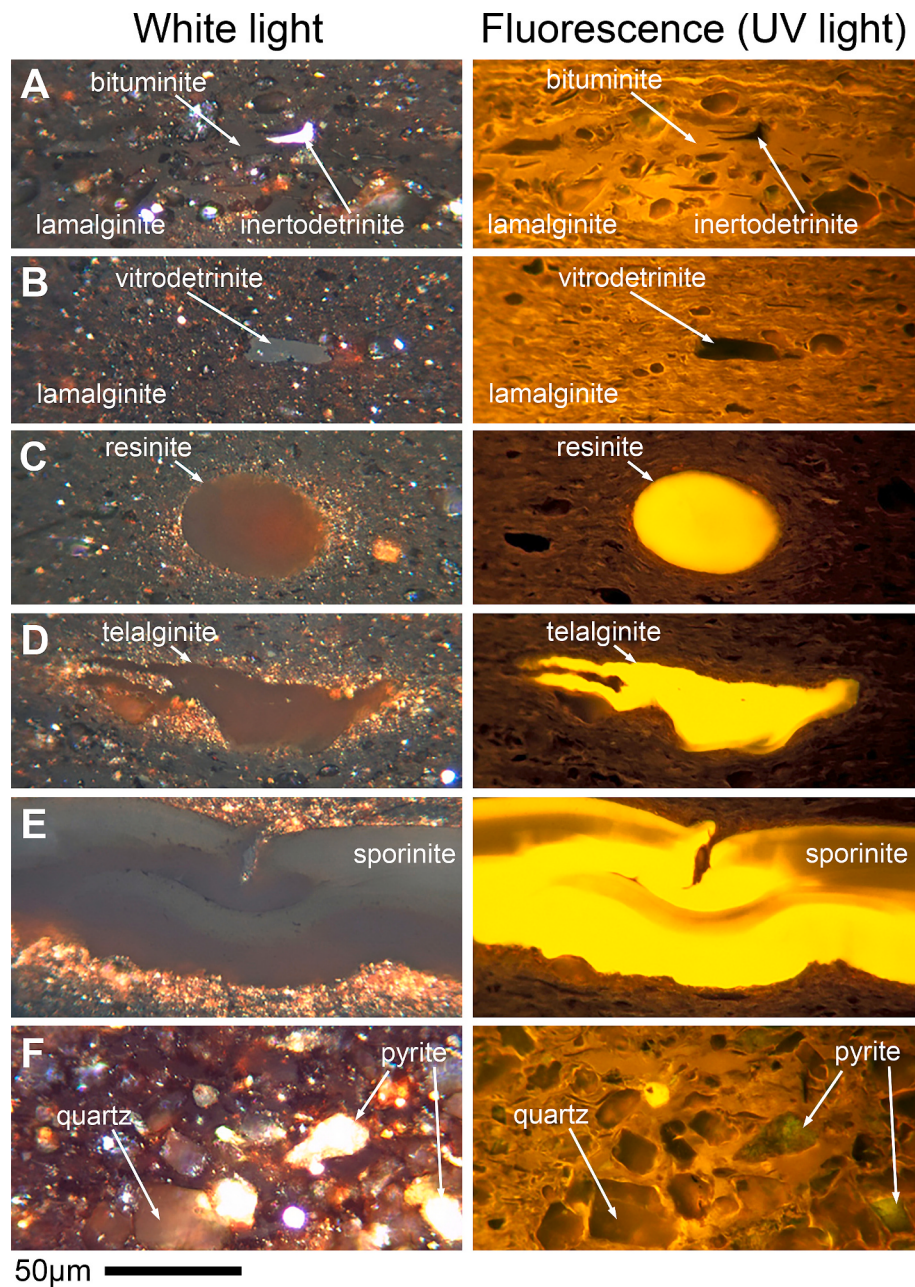


**Fig. 6.** Paired reflected light (left) and fluorescent (UV light, right) micrographs of black shale bed. Scale = 50  $\mu$ m. A. Bituminite and inertodetrinite embedded in matrix of lamalginite. B. Vitrodetrinite embedded in lamalginite. C. Resinate embedded of lamalginite. D. Telalginate embedded in lamalginite. E. Central portion of megasporite (sporinite) embedded in lamalginite. F. Mineral grains (quartz, pyrite) embedded in lamalginite.

**Table 2**

A. Vitrinite reflectance of fissile black shale.

Average Ro random	0.34	0.36
Maximum Ro random	0.38	0.47
Minimum Ro random	0.28	0.29
Standard Deviation	0.03	0.04
Calculated Ro maximum (Ro random * 1.066)	0.36	0.38

B. Composition of fissile black shale.

	As received	Dry
% Ash	50.61	51.12
% Mineral Matter	55.63	56.19
% Fixed Carbon	4.87	4.92
% Moisture	0.99	
% Volatile Matter	43.52	43.96
% Carbon	35.20	35.56
% Sulfur	1.76	1.78

composition in many respects is similar to the Spearfish assemblage. They are especially notable in the abundance of *Lueckisporites virkkiae*, as well as other more typically Lopingian Euramerican species such as *Jugasporites delasaucei* and *Klausipollenites schaubergeri* (Wilson, 1962; Morgan, 1967; Clapham Jr., 1970). Despite the somewhat precocious occurrence of taxa that are typically Lopingian, these three assemblages are distinct from their younger European counterparts in the DCA analysis, with the most disparate being one of the Flowerpot assemblages (Wilson, 1962). The El Reno Group palynofloras include many of the same taxa described from the late Permian, but also include relict Pennsylvanian taxa (*Triquitrites*, *Schopfipollenites*) and early Permian pollen forms (*Hamiapollenites*, *Potoneisporites*), supporting the inference of an earlier age for these assemblages. The age of the El Reno Group has been in contention, with interpretations shifting between early and middle Permian; however, several workers place it in the early middle Permian Roadian (Foster et al., 2014; Laurin and Hook, 2022).

Although the distance in ordination space between the Spearfish and other Pangaean North American assemblages is similar to those among several of the European assemblages, in general the Spearfish assemblage appears more similar to many of the Euramerican Lopingian palynofloras than to any of the middle Permian U.S. assemblages. This echoes our findings in the bilateral similarities between Spearfish and other assemblages (Fig. 8D). A close examination of common taxa among the four North American assemblages shows that only two species, *Rhizomaspora radiata* and *Clavatasporites irregularis* are common to the Spearfish assemblage and to at least one other U.S. assemblage. In contrast, the three El Reno Group assemblages include a number of taxa in common that do not occur in any Lopingian Euramerican assemblage, including *Alisporites aequus* L.R.Wilson, *Anguisporites contortus* L.R.Wilson, *A. intonsus* L.R.Wilson, *Calamospora breviradiata* Kosanke, *Hamiapollenites saccatus* L.R.Wilson, *H. tractiferinus* Jizba, *Hoffmeisterites (Potoneisporites) microdens* L.R.Wilson and *Vittatina lata* L.R.Wilson. These taxa share a common nomenclature among all three El Reno Group assemblages, but more importantly, they occur in early Permian palynofloras as well. The loss of taxa in the Spearfish assemblage that were also common in the Late Pennsylvanian and early Permian accounts for its difference with these early middle Permian palynofloras.

Palynofloras that are approximately coeval to middle Permian assemblages from the United States have also been described from the Canadian Arctic (Jansonius, 1962; Utting, 1994; Utting and Piasecki, 1995; Utting et al., 1997; Mangerud et al., 2021). These palynofloras

occur in the higher latitude Angaran biotic province, and are therefore significantly different in composition, so they were not included in the ordination. Although certain taxa are common to both Euramerican and Angaran phytoprovinces, such as species of *Lueckisporites*, *Lunatisporites*, *Scutaspores* and *Protohaploxylinus*, the Canadian Arctic floras include abundant and diverse species of *Hamiapollenites*, *Vittatina*, *Weylandites*, and *Cycadopites*, as well as diverse spore taxa (Utting, 1994; Utting and Piasecki, 1995; Utting et al., 1997). Jansonius (1962) described assemblages from the upper Belloy Formation of the Peace River embayment in western Canada that included *Vittatina* species, *Protohaploxylinus*, and notably *Hamiapollenites*; however, *Lueckisporites virkkiae* is absent. Dating of the upper Belloy Formation is somewhat uncertain, but conodont biostratigraphy indicates an age of Kungurian-Wordian (Henderson et al., 1994). The assemblage most closely resembling that of the Spearfish was briefly described from the Sadlerochit Formation on the North Slope of Alaska (Balme, 1980), who noted the presence of typical late Permian taxa *Klausipollenites schaubergeri*, *Lueckisporites virkkiae*, *Protohaploxylinus samoilovichii*, and *Striatoabietites richteri*, and compared the assemblage to Zechstein palynofloras. This assemblage was unfortunately never illustrated nor characterized in detail; however, invertebrates associated with the palynoflora are described as Kazanian (Roadian-early Wordian) in age (Balme, 1980).

## 5.2. Phytogeography and floristics

The Spearfish assemblage exhibits a high degree of taxonomic similarity to other regions of eastern Euramerica. Twenty-four morphotaxa identifiable to species level are present in late Permian floras of eastern Euramerica. In addition, other morphotaxa at the generic level have counterparts reported in the eastern Euramerican palynoflora. Only two morphotaxa, Genus A (Fig. 5.15) and *Clavatasporites irregularis* (Fig. 5.16), appear to have no counterpart elsewhere, indicating that endemism in this apparently isolated region was low. The Spearfish palynoflora indicates that the Lopingian Euramerican flora extended thousands of kilometers to the west from eastern Europe into western North America. Both spore diversity and abundance are very low, another characteristic shared by late Permian Euramerican palynofloras elsewhere.

Dispersed pollen indicates that the plants dominating the Spearfish assemblage were primarily voltzian conifers, peltasperms, and corystosperms. Some of the most abundant species in the palynoflora have been tied to specific members of the voltzian conifers. For example, pollen closely resembling *Lueckisporites virkkiae* has been found in situ in *Majonica alpina* pollen cones (Clement-Westerhof, 1987). This pollen form has also been hypothesized to be associated with another member of the Majonicaceae, *Pseudovoltzia liebeana* (Gibson et al., 2020). *Jugasporites delasaucei* is known from pollen cones of *Ullmannia frumentaria* (Potonié and Schweitzer, 1960). *Scutaspores unicus* has been associated with the Angaran conifer *Sashinia*, and *Vittatina* has been found in several peltasperm pollen organs (Gomankov and Meyen, 1986). Other pollen forms are less securely associated with specific groups. In the Euramerican and sub-Angaran phytoprovinces, multi-taeniate pollen, such as *Lunatisporites* and *Protohaploxylinus*, are generally associated with late Permian peltasperms (Gomankov and Meyen, 1986; Meyen, 1997; Zavialova and Karasev, 2015). The morphologically very similar form genera *Falcisporites* and *Alisporites* have been tied to a variety of corystosperm and peltasperm seed ferns (Zavada and Crepet, 1985; Balme, 1995; Lindström et al., 1997; Nau-golnykh, 2013). Late Permian *Vesicaspora* most likely represents peltasperms (Kerp, 1988; Krassilov et al., 1999; Zavialova, 2011), whereas

**Table 3**

Carbon and oxygen isotope values for black shale bed.

Sample	$\delta^{13}\text{C}$ (‰) PDB	$\delta^{18}\text{O}$ (‰) PDB
S1A1A: micrite in phylloid algal packstone	-5.72	4.70
S1A1B: micrite in phylloid algal packstone	-5.65	4.58
S1A2-1: microbialite clast in anhydrite-cemented mudstone/skeletal wackestone	-1.25	3.21
S1A2-2: microbialite clast	-1.17	3.26
S1B2: microbialite mudstone/wackestone	-1.69	2.84

other forms, such as *Klausipollenites*, have not been linked to specific taxa, but likely represent conifers or peltasperms. With respect to spores, *Cyclogranisporites* is a generalized morphotaxon that could be produced by any of number of ferns in the Polypodiopsida (sensu PPG1), but is often associated with members of the Marattiales in Pennsylvanian and Permian floras (Balme, 1995 and references therein). *Clavatasporites irregularis* is of unknown affinity, but could represent a pteridophyte or a moss (the latter group tends to lack clear germinal apertures). A complete list of botanical affinities may be found in Table 4.

### 5.3. Depositional environment of the 'black shale bed'

The carbonate facies associated with the palynoflora indicate deposition in a poorly circulated, shallow water environment that underwent episodic evaporative drawdown and exposure leading to surface brecciation. The pervasive micropeloidal textures, interpreted as microbially mediated, indicate mat-forming algae or cyanobacteria, which would have grown in the upper photic zone. The possible presence of *Archaeolithophyllum*, a coralline red alga, could indicate somewhat deeper water or episodic flooding of the depositional environment by marine waters. Weakly developed pedogenic alteration in one sample indicates exposure and incipient soil development. The packstones and wackestones that include invertebrate skeletal grains are typical of shallow-water lagoons distal from active distributary channels in modern sabkha settings, as are cyanobacterial coated grains (Warren, 2006). Abundant gypsum (after anhydrite) cements that occlude primary porosity and secondary porosity created by surface brecciation likely formed in shallow evaporative pans on a sabkha that were episodically filled with seawater and/or saline continental brines. The presence of gypsum cements in several samples, as well as the stable isotopic composition of the carbonates, support deposition under highly evaporative conditions.

The microbialite clasts were cemented syndepositionally and, therefore, are reliable records of the isotopic composition of the fluid from which they precipitated. The  $\delta^{18}\text{O}$  values of microbialite clasts are

significantly elevated compared to normal marine water, and require evaporation of seawater. This is a finding compatible with the prevalence of gypsum after anhydrite cements in primary and secondary porosity in these carbonates. Today, and in the recent past, such high values are typical of the Persian Gulf sabkha flats. Conversely, the  $\delta^{13}\text{C}$  values of the micropeloidal mudstone/wackestone (-1.7 to -1.2 ‰) and phylloid algal packstone (-5.7 ‰ ± 0.3 ‰) are lower, to significantly lower, than typical marine values of Permian open-marine carbonates, which were about ~ +4 ‰ ± 2 ‰ (Cramer and Jarvis, 2020). This finding is compatible with microbially mediated and algal carbonates that are enriched in  $^{12}\text{C}$  through photosynthesis.

The dominance of the maceral lamalginitite indicates an algal source for most of the organic matter in the black shale. Such a source points to an open water depositional environment with minimal system energy, and minimum clastic input. Therefore, the setting is likely an embayment or lagoon. The relatively low sulfur content of the shale (1.8 %) indicates that the water column was fresh or possibly brackish, but probably not fully marine at the time of accumulation. The paucity of "terrestrial" macerals (e.g., vitrinite, inertinite, sporinite) may indicate that areas adjacent to the open water system were sparsely vegetated. The high TOC content (34 %) indicates oxygen-starved conditions under which the preservation of organic matter was promoted. High surface-water temperatures would have contributed to a low oxygen regime. However, the water column must have been sufficiently stratified with enough oxygen to promote abundant algal growth at the sediment-water interface, and deeper dysoxic to anoxic layers, which preserved a large proportion of the organic material. Alternatively, the presence of a low diversity acritarch flora in the gray siltstone subjacent to the lamalginitite may indicate a brackish, rather than freshwater, embayment, conducive to algal growth but perhaps restricted to taxa tolerant of fluctuating or higher salinity.

Quartz grains in the black shale and underlying gray siltstone are clearly eolian in origin. Evidence supporting this interpretation includes the fact that virtually all quartz grains demonstrate angularity. Some outer amorphous grain surfaces show evidence of dissolution and replacement by recrystallized chert interpreted to represent etched surfaces with a secondary coating of chert (Cecil et al., 2018). Spearfish deposition occurred at ~10–12 degrees north of the paleoequator, indicating deposition at the southern boundary of the Northern Hemisphere where prevailing easterly trade winds operated. Furthermore, Spearfish deposition occurred west of the high Appalachian chain, placing the region in the rain shadow (and wind shadow) of these mountains. Combined evidence from quartz grains, palynology, carbonate isotope geochemistry, and organic petrography, associated with extensive evaporite deposits, all point to a setting under substantial aridity during the time of Spearfish deposition.

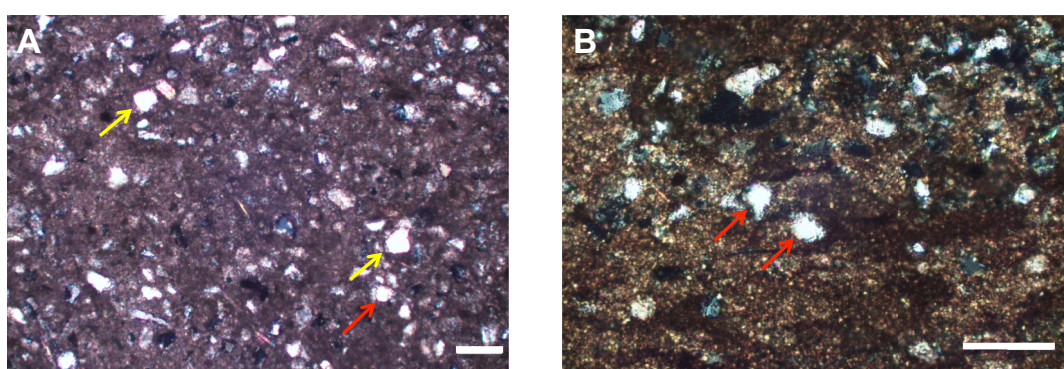
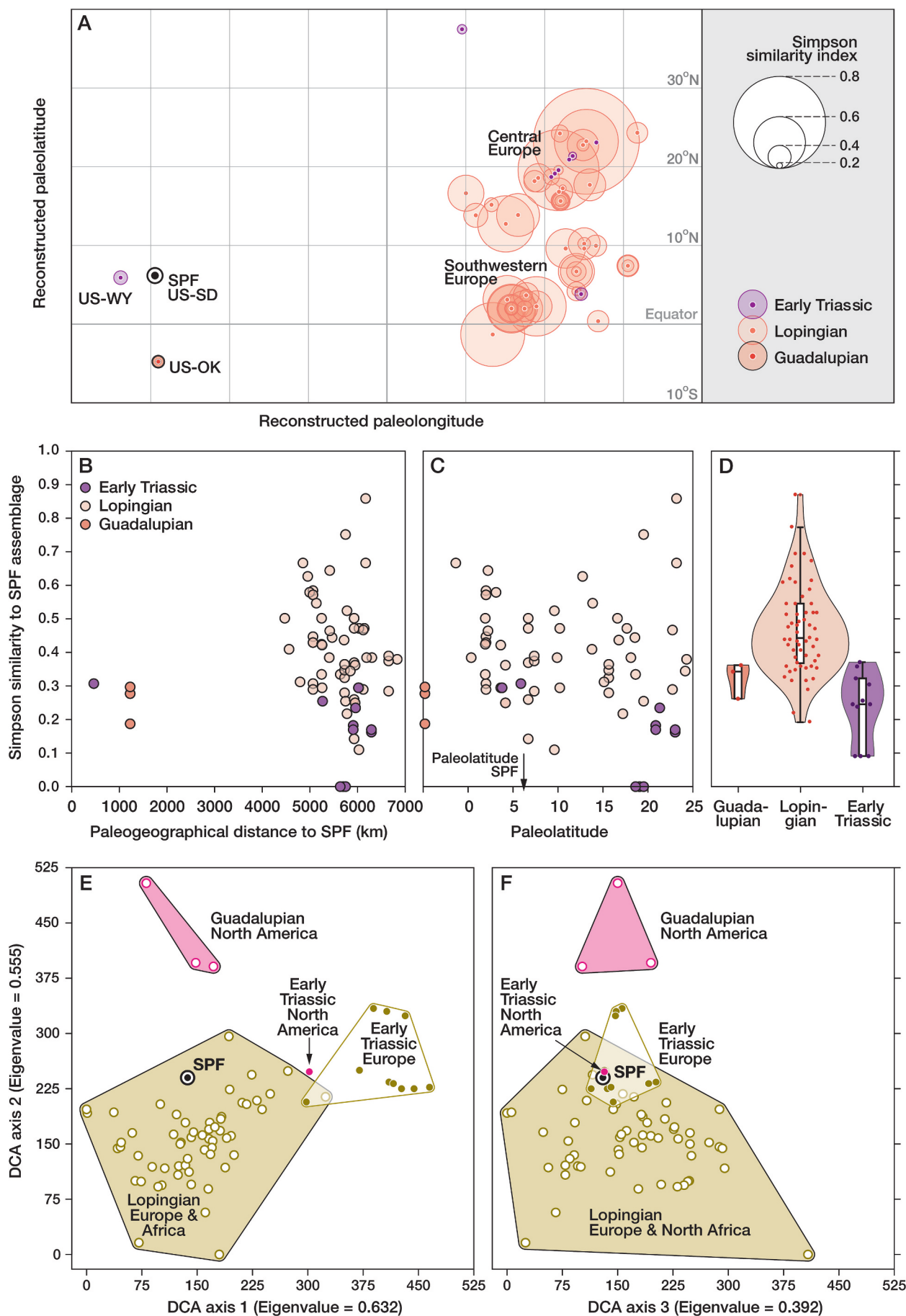


**Fig. 7.** Thin section micrographs under Crossed Nicols. Scale is 100 µm. A. Loessite underlying the black shale bed (USNM 43663-1-loessite). Yellow arrows indicate coarse quartz silt exhibiting serrated rims resulting from dissolution of disordered lattice. Red arrow indicates medium quartz silt grain showing both a serrated edge and chert overgrowth. B. Pollen-bearing mudstone at base of fissile carbonaceous shale (USNM 43663-3-mudstone). Red arrows denote white grains of eolian quartz grains with deeply serrated edges and with minor authigenic chert. (For interpretation of the references to colour in this figure legend, the reader is referred to the web version of this article.)



(caption on next page)

**Fig. 8.** Comparison of palynofloral assemblages. The Spearfish assemblage (SPF) was compared to 72 palynofloras from the same low-latitudinal zone in central Pangaea, comprising 3 Guadalupian, 58 Lopingian, and 11 Early Triassic assemblages. Simpson similarity indices (bilaterally comparing each palynoflora to the Spearfish assemblage) have been plotted geographically according to their reconstructed paleolocation in the Lopingian (A). Diameter of the circles scales with the squared similarity index value for each location. Similarity values have also been plotted against their paleogeographical distance to the Spearfish locality (B) and their paleolatitude (C). The similarity index frequency distributions per Epoch (D) is visualized as a combination of box plots (showing the within-Epoch interquartile range and median), violin plots (approximating a probability density function of the data distribution) and the individual data points shown as jitter plot overlay. The ordination of palynofloras along the first three axes of a Detrended Correspondence Analysis (E, F) reveals the main types of taxonomic-compositional change among all assemblages, binned by geographic region and Epoch.

#### 5.4. Taphonomy of dispersed palynomorphs

Every palynological assemblage is filtered through taphonomic processes, thereby complicating interpretation of its floristic signal. There is an extensive literature on taphonomy of modern pollen in lake environments, which the Spearfish assemblage most closely resembles. In general, low-statured plants such as pteridophytes contribute proportionately less to an assemblage compared to wind-pollinated canopy height trees (Scheibling, 1980), which could in part account for the very low percentage of spores in the Spearfish. Other factors potentially influencing the composition of the Spearfish assemblage include vegetation openness (open vs. closed canopy forests vs. scrub vegetation), pollen productivity, whether wind or water was more important in depositing grains, and distance from site of deposition. These factors are unfortunately largely unknown for the Spearfish assemblage. One notable aspect of the assemblage is that all but five of the species are saccate. Saccate pollen floats longer distances in water (Farley, 1990), which could potentially contribute to over-representation in the assemblage. However, it should be kept in mind that most known

Permian seed plants produced saccate pollen, so this factor is also difficult to assess. The small sample size (only 300 grains) will miss less common forms that might contribute to a more complete view of the vegetation. Regardless, spore-bearing plants (ferns, lycophytes, bryophytes) representing primarily hydrophilic to mesophilic plants are largely absent from the Spearfish assemblage. Even given taphonomic biases, the composition of the palynological assemblages supports sedimentological and isotopic evidence of a very warm and dry climate.

#### 6. Conclusions

- The lower portion of the Spearfish Formation of South Dakota is firmly established as late Permian (Lopingian) on the basis of a single palynological assemblage.
- The Spearfish palynofloral assemblage represents the first plant fossils of any kind described from the late Permian (Lopingian) in North America.
- The Spearfish assemblage closely resembles those of Lopingian European palynofloras of the low latitude Euramerican floral province,

**Table 4**  
Botanical affinities of dispersed pollen and spores (in alphabetical order).

Pollen genus/species	Parent plant	Age	Reference
<i>Corisaccites altus</i>	Unknown conifer or peltasperm	Permian-Triassic	
<i>Falcisporites/</i> <i>Alisporites</i>	<i>Pterispermstrobus</i>	Permian	Balme (1995); Zavialova & Van Konijnenburg-van Cittert (2011)
<i>Falcisporites/</i> <i>Alisporites</i>	<i>Ullmannia</i>	Permian	Florin (1944); Potonié (1962)
<i>Falcisporites/</i> <i>Alisporites</i>	Corystospermales, peltasperm	Permian-Triassic	Zavada and Crepet (1985); Balme (1995); Lindström et al. (1997); Naugolnykh (2013)
<i>Fuldaesporites</i> sp.	Unknown conifer or peltasperm	Permian	
<i>Jugasporites delasauciei</i>	<i>Ullmannia frumentaria</i> (voltzian conifer)	late Permian	Potonié and Schweitzer (1960)
<i>Jugasporites</i> spp.	?voltzian conifer	Permian-Triassic	
<i>Klausipollenites</i>	Unknown conifer or peltasperm	Permian-Triassic	
<i>Limitisporites</i>	Unknown conifer or peltasperm	Permian-Triassic	
<i>Lueckisporites virkkiae</i>	<i>Majonica alpina</i> (voltzian conifer)	mid-late Permian	Clement-Westerhof (1987)
<i>Lunatisporites</i>	Peltaspermales	Permian	Gomankov and Meyen (1986)
<i>Lunatisporites</i>	Unknown conifer or peltasperm	late Permian	Clement-Westerhof (1974)
<i>Nuskoisporites</i>	<i>Ortiseia</i> (walchian conifer)	mid-late Permian	Poort et al. (1997)
<i>Paravesicaspora</i>	(see <i>Vesicaspora</i> )	Permian	
<i>Pityosporites devolvens</i>	Unknown conifer or peltasperm	Permian	
<i>Platysaccus</i>	Unknown conifer or seed fern	Pennsylvanian-Permian	
<i>Protohaploxylinus</i>	<i>Peltaspermopsis</i> ( <i>Tatarina</i> ), <i>Permotheca striatifera</i> (peltasperm)	Permian	Gomankov and Meyen (1986); Zavialova and Karasev (2015)
<i>Rhizomaspora radiata</i>	Unknown conifer or peltasperm	Permian	
<i>Scutaspores unicus</i>	<i>Dvinostrobus</i> ; <i>Sashinia/Quadrocladus</i>	late Permian	Klaus (1963); Gomankov and Meyen (1986)
<i>Striatobaeites</i>	Unknown conifer or peltasperm	Permian	
<i>Strotersporites jansonii</i>	Unknown conifer or peltasperm	Permian	
<i>Vesicaspora</i>	<i>Pterispermstrobus</i> (peltasperm)	early-late Permian	Gomankov and Meyen (1986); Kerp (1988); Barthel (2006)
<i>Vesicaspora</i>	<i>Permotheca</i> (peltasperm)	early Permian	Krassilov et al. (1999)
<i>Vesicaspora</i>	<i>Permotheca vesicasporoides</i>	late Permian	Gomankov and Meyen (1986); Zavialova & Van Konijnenburg-van Cittert (2011)
<i>Vittatina</i>	<i>Peltaspermopsis buevichiae</i> , <i>Permotheca vittitinifera</i> , <i>Salpingocarpus</i> (peltasperms)	late Permian	Gomankov and Meyen (1986)
<b>Spore genus/species</b>			
<i>Clavatasporites irregularis</i>	unknown	early-late Permian	
<i>Cyclogranisporites</i>	Marattiales	Carboniferous-Mesozoic	Lesnikowska (1989); Balme (1995)

- and especially those near the Zechstein sea that extended from Eastern and Northern Europe into the Italian Alps and westward into Great Britain and Ireland. These assemblages reflect a homogeneous conifer- and peltasperm-rich, xeric adapted flora, depauperate in pteridophytes, that extended thousands of miles into North America, reflecting widespread warming of the planet in the late Permian.
- Similar palynofloral assemblages from the Guadalupian of Oklahoma indicate warming was well underway by mid Permian times in low latitude North America.
  - The rare organic-rich unit preserving the Spearfish assemblage represents a restricted basin, perhaps an embayment or lagoon, in an arid coastal sabkha setting.

## Dedication

Our coauthor Blaine Cecil passed away during the final preparation of this paper. Blaine was a person from whom ideas and insights flowed freely up to the end of his life. He never stopped asking questions and, through the sharing of his thoughts and insights, greatly influenced all of us who worked with him. Personally, Blaine was a gentleman of the old school, polite, respectful, and with a firm, clear sense of right, wrong, and responsibility. A man of great accomplishment, he was modest to the core. His friendship and wisdom will be greatly missed.

## CRediT authorship contribution statement

**Carol L. Hotton:** Conceptualization, Validation, Project administration, Methodology, Investigation, Data curation, Visualization, Writing – original draft. **Antoine Bercovici:** Conceptualization, Validation, Formal analysis, Methodology, Investigation, Visualization, Writing – review & editing. **Cindy V. Looy:** Conceptualization, Validation, Investigation, Visualization, Writing – review & editing. **Ivo A.P. Duijnsteet:** Formal analysis, Methodology, Investigation, Validation, Visualization, Writing – review & editing. **Dan S. Chaney:** Investigation, Visualization, Resources, Writing – review & editing. **Cortland F. Eble:** Formal analysis, Methodology, Investigation, Visualization, Writing – review & editing. **Isabel P. Montañez:** Methodology, Formal analysis, Investigation, Writing – review & editing. **Sylvie Bourquin:** Methodology, Formal analysis, Investigation, Visualization, Writing – review & editing. **Blaine Cecil:** Formal analysis, Investigation, Visualization, Writing – review & editing. **John Nelson:** Methodology, Investigation, Writing – review & editing. **Robert A. Gastaldo:** Methodology, Investigation, Writing – review & editing. **Johnathan Wingerath:** Investigation, Resources, Writing – review & editing. **William A. DiMichele:** Conceptualization, Funding acquisition, Investigation, Resources, Writing – review & editing.

## Declaration of competing interest

The authors declare that they have no known competing financial interests or personal relationships that could have appeared to influence the work reported in this paper.

## Acknowledgements

The fieldwork on which this study is based was supported by a grant from the Smithsonian National Museum of Natural History small grants program. The research of Carol Hotton was supported in part by the Intramural Research Program of the National Institutes of Health, National Library of Medicine. We are grateful to Rob Wardell for help with petrographic photography. We thank Howard Falcon-Lang, Evelyn Kustatscher and an anonymous reviewer for their helpful suggestions and comments that greatly improved the manuscript.

## Appendix A. Supplementary data

Supplementary data to this article can be found online at <https://doi.org/10.1016/j.palaeo.2025.113218>.

## Data availability

Data will be made available on request.

## References

- Archangelsky, S., 1990. Plant distribution in Gondwana during the late Paleozoic. In: Taylor, E.L., Taylor, T.N. (Eds.), Antarctic Paleobiology. Springer-Verlag, New York, pp. 102–117.
- Balme, B.E., 1980. Palynology of late Permian-early Triassic strata in Greenland and Alaska, and its plant geographic implications. In: 5<sup>th</sup> International Palynological Conference, Cambridge, Abstract, p. 25.
- Balme, B.E., 1995. Fossil *in situ* spores and pollen grains: an annotated catalogue. Rev. Palaeobot. Palynol. 87, 81–323.
- Behnken, F.H., 1975. Leonardian and Guadalupian (Permian) conodont biostratigraphy in western and southwestern United States. J. Paleontol. 49, 284–315.
- Behnken, F.H., Wardlaw, B.R., Stout, L.N., 1986. Conodont biostratigraphy of the Permian Meade Peak phosphatic shale member, Phosphoria Formation, southeastern Idaho. Rocky Mountain Geology 24, 169–190.
- Bernardi, M., Petti, F.M., Kustatscher, E., Franz, M., Hartkopf-Fröder, C., Labandeira, C.C., van Konijnenburg Wappler, T., van Cittert, J.H.A., Peecock, B.R., Angelczy, K.D., 2017. Late Permian (Lopingian) terrestrial ecosystems: a global comparison with new data from the low-latitude Bletterbach Biota. Earth Sci. Rev. 175, 18–43.
- Boyd, D.W., 1993. Paleozoic history of Wyoming. In: Snee, A.W., Steidtmann, J.R., Roberts, S.M. (Eds.), Geology of Wyoming, Geol. Surv. Wyoming Mem., Vol. 5, pp. 164–187.
- Cecil, C.B., Hemingway, B.S., Dulong, F.T., 2018. The chemistry of eolian quartz dust and the origin of chert. J. Sediment. Res. 88, 743–752.
- Choi, S.S., Cha, S.H., Tappert, C.C., 2010. A survey of binary similarity and distance measures. J. Syst. Cybern. Inform. 8, 43–48.
- Clapham Jr., W.B., 1970. Permian miospores from the flowerpot formation of western Oklahoma. Micropaleontology 16, 15–36.
- Clement-Westerhof, J.A., 1974. *In situ* pollen from gymnospermous cones from the upper Permian of the Italian Alps - a preliminary account. Rev. Palaeobot. Palynol. 17, 63–73.
- Clement-Westerhof, J.A., 1987. Aspects of Permian palaeobotany and palynology. VII. The Majonicaceae, a new family of late Permian conifers. Rev. Palaeobot. Palynol. 52, 375–402.
- Cramer, B.D., Jarvis, I., 2020. Chapter 11 - Carbon isotope stratigraphy. In: Gradstein, F.M., Ogg, J.G., Schmitz, M.D., Ogg, G.M. (Eds.), The Geologic Time Scale 2020. Elsevier, pp. 309–342.
- Cuneo, N.R., 1996. Permian phytogeography in Gondwana. Palaeogeogr. Palaeoclimatol. Palaeoecol. 125, 75–104.
- Darton, N.H., 1899. Jurassic formations of the Black Hills of South Dakota. Geol. Soc. Am. Bull. 10, 383–396.
- Darton, N.H., 1901. Geology and water resources of the southern half of the Black Hills and adjoining regions in South Dakota and Wyoming. U.S. Geol. Surv. 21<sup>st</sup> Ann Rep. 4, 489–599.
- DiMichele, W.A., Hook, R.W., Nelson, W.J., Chaney, D.S., 2004. An unusual Middle Permian flora from the Blaine Formation (Pease River Group: Leonardian-Guadalupian Series) of King County, West Texas. J. Paleontol. 78, 765–782.
- DiMichele, W.A., Kerp, H., Tabor, N.J., Looy, C.V., 2008. The so-called “Paleophytic-Mesophytic” transition in equatorial Pangea - Multiple biomes and vegetational tracking of climate change through geological time. Palaeogeogr. Palaeoclimatol. Palaeoecol. 268, 152–163.
- DiMichele, W.A., Looy, C.V., Chaney, D.S., 2011. A new genus of gigantopterid from the middle Permian of the United States and China and its relevance to the gigantopterid concept. Int. J. Plant Sci. 172, 107–119.
- Farley, M.B., 1990. Vegetation distribution across the early Eocene depositional landscape from palynological analysis. Palaeogeogr. Palaeoclimatol. Palaeoecol. 79, 11–27.
- Florin, R., 1944. Die koniferen des oberkarbons und des unteren perms. Palaeontogr. Abt. B 85, 365–456.
- Foster, T.M., Soreghan, G.S., Soreghan, M.J., Benison, K.C., Elmore, R.D., 2014. Climatic and paleogeographic significance of eolian sediment in the middle Permian Dog Creek Shale (Midcontinent U.S.). Palaeogeogr. Palaeoclimatol. Palaeoecol. 402, 12–29.
- Gibson, M.E., Taylor, W.A., Wellman, C.H., 2020. Wall ultrastructure of the Permian pollen grain *Lueckisporites virkiae* Potonié et Klaus 1954 emend. Clarke: evidence for botanical affinity. Rev. Palaeobot. Palynol. 275, 104169.
- Gomankov, A.V., Meyen, S.V., 1986. Татарина-флора (состав, распространение в поздней перми Евразии). [Tatarian flora (composition and distribution in the late Permian of Eurasia)]. Trans. Geol. Inst. Acad. Sci. USSR 401, 1–173 (in Russian).
- Hagadorn, J.W., Whiteley, K.R., Lahey, B.L., Henderson, C.M., Holm-Denoma, C.S., 2016. The Permian-Triassic transition in Colorado. In: Keller, S.M., Morgan, M.L. (Eds.), Unfolding the Geology of the West: Geol. Soc. Amer. Field Guide, Vol. 44, pp. 73–92.
- Hammer, Ø., Harper, D.A., 2001. Past: paleontological statistics software package for education and data analysis. Palaeontol. Electron. 4, 1.

- Henderson, C.M., 2018. Permian conodont biostratigraphy. In: Lucas, S.G., Shen, S.Z. (Eds.), The Permian Timescale. Geol. Soc. London Spec. Publ. Vol. 450, pp. 119–142.
- Henderson, C.M., Richards, B.C., Barclay, J.E., 1994. Permian Strata of the Western Canada Sedimentary Basin. In: Mossop, G., Shetsen, I. (Eds.), Atlas of the Western Canada Sedimentary Basin. Canadian Society of Petroleum Geologists, Calgary, Alberta, Canada and Alberta Research Council, Edmonton, Alberta Canada.
- Jansonius, J., 1962. Palynology of Permian and Triassic sediments, Peace River Area, Western Canada. Palaeontogr. Abt. B 110, 35–98.
- Johnson, E.A., 1993. Depositional history of Triassic rocks in the area of the Powder River Basin, northeastern Wyoming and southeastern Montana. U.S. Geol. Surv. Bull. 1917, 1–30.
- Kerp, J.H.F., 1988. Aspects of Permian palaeobotany and palynology. X. The Western and central European species of the genus *Autunia* Krässer emend. Kerp (Peltaspermaceae) and the form genus *Rhachiphyllum* Kerp (callipterid foliage). Rev. Palaeobot. Palynol. 54, 249–360.
- Klaus, W., 1963. Sporen aus dem sudalpinen Perm. Jahrb. Geol. Bundesanst. 106, 229–363.
- Krassilov, V.A., Afonin, S.A., Naugolnykh, S.V., 1999. *Permotheca* with *in situ* pollen grains from the lower Permian of the Urals. Palaeobotany 48, 19–25.
- Kürschner, W.M., Herngreen, G.F.W., 2010. Triassic palynology of central and northwestern Europe: a review of palynofloral diversity patterns and biostratigraphic subdivisions. Geol. Soc. London Spec. Publ. 334, 263–283.
- Kustatscher, E., van Konijnenburg van Cittert, J.H.A., Looy, C.V., Labandeira, C.C., Wappler, T., Butzmann, R., Fischer, T.C., Krings, M., Kerp, H., Visscher, H., 2017. The Lopingian (late Permian) flora from the Bletterbach Gorge in the Dolomites, Northern Italy: a review. Geol. Alp. 14, 39–60.
- Laurin, M., Hook, R.W., 2022. The age of North America's youngest Paleozoic continental vertebrates: a review of data from the Middle Permian Pease River (Texas) and El Reno (Oklahoma) groups. Earth Sci. Bull. 193 (10), 1–30.
- Lesnikowska, A.D., 1989. Anatomically Preserved Marattiales from Coal Swamps of the Desmoinesian and Missourian of the Midcontinent United States: Systematics, Ecology and Evolution. PhD thesis. University of Illinois, Urbana, Illinois, U.S.A., pp. 1–227.
- Li, X., Yao, Z., 1982. A review of recent research on the Cathaysia flora in Asia. Amer. J. Bot. 69, 479–486.
- Lindberg, F.A., 1988. Central and Southern Rockies Region: American Association of Petroleum Geologists, Correlation of Stratigraphic Units of North America (COSUNA) Project, 1 Sheet.
- Lindström, S., McLoughlin, S., Drinnan, A.N., 1997. Intraspecific variation of taeniate bisaccate pollen within Permian glossoperid sporangia, from the Prince Charles Mountains, Antarctica. Int. J. Plant Sci. 158, 673–684.
- Looy, C.V., Duijnstee, I.A.P., 2020. Voltzian conifers of the South Ash Pasture flora (Guadalupian, Texas): *Johniphylloides multirerve* gen. Et sp. nov., *Pseudovoltzia sapflorensis* sp. nov., and *Wantus acaulis* sp. nov. Int. J. Plant Sci. 181, 363–385.
- Mangerud, G., Paterson, N.W., Bujak, J., 2021. Permian palynoevents in the circum-Arctic region. Atl. Geol. 57, 57–69.
- Meyen, S.V., 1982. The Carboniferous and Permian floras of Angaraland (a synthesis). Biol. Membr. 7, 1–109.
- Meyen, S.V., 1987. Fundamentals of Paleobotany. Chapman and Hall, London, New York, pp. 1–432.
- Meyen, S.V., 1997. Permian conifers of western Angaraland. Rev. Palaeobot. Palynol. 96, 351–447.
- Morgan, B.E., 1967. Palynology of a Portion of the El Reno Group (Permian), Southwest Oklahoma. University of Oklahoma, pp. 1–129. Ph.D. Dissertation.
- Müller, R.D., Cannon, J., Qin, X., Watson, R.J., Gurnis, M., Williams, S., Pfaffelmoser, T., Seton, M., Russell, S.H., Zahirovic, S., 2018. GPlates: building a virtual Earth through deep time. Geochem. Geophys. Geosyst. 19, 2243–2261.
- Naugolnykh, S.V., 2013. New male reproductive organs of gymnosperms *Permotheca colovratica* sp. nov. from the lower Permian of the Ural Mountains. Paleontol. J. 47, 114–126.
- Nowak, H., Schneebeli-Hermann, E., Kustatscher, E., 2018. Correlation of Lopingian to Middle Triassic Palynozones. J. Earth Sci. 29, 755–777.
- Paul, R.K., Paul, R.A., 1983. Revision of type lower Triassic Dinwoody Formation, Wyoming, and designation of principal reference section. Rocky Mountain Geol. 22, 83–90.
- Port, R.J., Clement-Westerhof, J.A., Looy, C.V., Visscher, H., 1997. Aspects of Permian palaeobotany and palynology. XVII. Conifer extinction in Europe at the Permian-Triassic junction: morphology, ultrastructure and geographic/stratigraphic distribution of *Nuskiosporites duthunyi* (prepollen of *Ortiseia*, Walchiaceae). Rev. Palaeobot. Palynol. 97, 9–39.
- Potonié, R., 1962. Synopsis der Sporae *in situ*. Beih. Geol. Jahrb. 52, 1–204.
- Potonié, R., Schweitzer, H.-J., 1960. Der pollen von *Ullmannia frumentaria*. Paläontol. Z. 34, 27–39.
- Rees, P.M., Ziegler, A.M., Gibbs, M.T., Kutzbach, J.E., Behling, P.J., Rowley, D.B., 2002. Permian phytogeographic patterns and climate data/model comparisons. J. Geol. 110, 1–31.
- Robinson, C.S., Mapel, W.J., Bergendahl, M.H., 1964. Stratigraphy and structure of the northern and western flanks of the Black Hills Uplift, Wyoming, Montana, and South Dakota. U.S. Geol. Surv. Prof. Pap. 404, 1–134.
- Sabel, J.M., 1984. Sedimentology and depositional history of the Permo-Triassic Spearfish Formation, southwestern Black Hills, South Dakota. The Permian and Pennsylvanian Geology of Wyoming. Wyoming Geol. Soc Guidebook 35, 295–307.
- Scheibling, M.H., 1980. Reduction of wind velocity by the forest canopy and the rarity of non-arborescent plants in the Upper Carboniferous fossil record. Argum. Palaeobot. 6, 133–138.
- Schweitzer, H.J., 1986. The land flora of the English and German Zechstein sequences. In: Harwood, G.M., Smith, D.B. (Eds.), The English Zechstein and Related Topics, 22. Geol. Soc. Spec. Pub., Oxford, pp. 31–54.
- Stack, J., Gottfried, M.D., 2021. A new, exceptionally well-preserved Permian actinopterygian fish from the Minnekahta Limestone of South Dakota, USA. J. Syst. Palaeontol. 19, 1271–1302.
- Teichmüller, M., 1974. Über neue macreral der Liptinit-Gruppe und die Entstehung von Micrinit. Fortschr. Geol. Rheinl. Westfalen 24, 37–64.
- Ter Braak, C.J., 1985. Correspondence analysis of incidence and abundance data: properties in terms of a unimodal response model. Biometrics 41, 859–873.
- Uhl, D., Kerp, H., 2020. Die terrestrische Makroflora des Zechsteins. In: Deutsche Stratigraphische Kommission (Hrsg.); Koordination und Redaktion: J. Paul & H. Hegemann für die Subkommission Perm-Trias): Stratigraphie von Deutschland XII. Zechstein, Schriftenreihe der Deutschen Gesellschaft für Geowissenschaften, Berlin 89, 83–91.
- Utting, J., 1994. Palynostratigraphy of Permian and lower Triassic rocks, Sverdrup Basin, Canadian Arctic Archipelago. Geol. Surv. Can. Bull. 478, 1–118.
- Utting, J., Piasecki, S., 1995. Palynology of the Permian of northern Continents: A review. In: Scholle, P.A., Peryt, T.M., Ulmer-Scholle, P.A. (Eds.), The Permian of Northern Pangea, Volume 1. Palaeogeography, Palaeoclimates, Stratigraphy. Springer, Berlin, pp. 236–261.
- Utting, J., Esaulova, N.K., Silantiev, V.V., Makarova, O.V., 1997. Late Permian palynomorph assemblages from Ufimian and Kazanian type sequences in Russia, and comparison with Roadian and Wordian assemblages from the Canadian Arctic. Can. J. Earth Sci. 34, 1–16.
- Wang, Z., 1985. Palaeovegetation and plate tectonics: palaeophytogeography of North China during Permian and Triassic times. Palaeogeogr., Palaeoclimatol., Palaeoecolgy 49, 25–45.
- Wardlaw, B.R., 2015. Gondolellid conodonts and depositional setting of the Phosphoria Formation. Micropaleontology 61, 335–368.
- Wardlaw, B.R., Collinson, J.W., 1979. Biostratigraphic zonation of the Park City Group. U.S. Geol. Surv. Prof. Pap. 1163, 17–22.
- Wardlaw, B.R., Collinson, J.W., 1986. Paleontology and deposition of the Phosphoria Formation. Rocky Mtn. Geol. 24, 107–142.
- Warren, J.K., 2006. Evaporites: Sediments. Resources and Hydrocarbons. Springer-Verlag, Berlin Heidelberg, pp. 1–1036.
- Wilson, L.R., 1962. Plant microfossils from the Flowerpot Formation. Oklahoma Geol. Notes, Circ. 49, 1–50.
- Zahirovic, S., Eleish, A., Doss, S., Pall, J., Cannon, J., Pistone, M., Tetley, M.G., Young, A., Fox, P., 2022. Subduction and carbonate platform interactions. Geosci. Data J. 9, 371–383.
- Zavada, M.S., Crepet, W.L., 1985. Pollen wall ultrastructure of the type material of *Pteruchus africanus*, *P. Dubius* and *P. Papillatus*. Pollen Spores 27, 271–276.
- Zavialova N, van Konijnenburg-van Cittert, J.H.A., 2011. Exine ultrastructure of *in situ* peltasperm pollen from the Rhaetian of Germany and its implications. Rev. Palaeobot. Palynol. 168, 7–20.
- Zavialova, N., Karasev, E., 2015. Exine ultrastructure of *in situ* *Protohaploxylinus* from a Permian peltasperm pollen organ, Russian Platform. Rev. Palaeobot. Palynol. 213, 27–41.